Studies of Gas Disks in Binary Systems

Studies of Gas Disks in Binary Systems

Miguel de Val-Borro

Stockholm University

ISBN 978-91-7155-776-6

Printed in Sweden by US-AB, Stockholm 2008

Distributor: Astronomy Department, Stockholm University

Para mi familia

Abstract

Until 1995 our theories of planet formation were based on our knowledge of the planets in the Solar System. Now there have been over 300 extrasolar planets detected through radial velocity surveys and photometric studies, showing a tremendous variety of masses, compositions and orbital parameters. Understanding the way these exoplanets formed and evolved within the circumstellar disks they were initially embedded in is a crucial and very timely issue. The interaction between a protoplanet and a disk cannot be fully understood analytically and hydrodynamic simulations are needed. In the first part of this thesis we study the physical interaction between a gaseous protoplanetary disk and an embedded planet using numerical simulations. In order to trust the results from simulations it is important to compare different numerical methods. However, the standard test problems for hydrodynamic codes differ considerably from the case of a protoplanetary disk interacting with an embedded planet. We have carried out a code comparison in which the problem of a massive planet in a protoplanetary disk was studied with various numerical schemes. We compare the surface density, potential vorticity and azimuthally averaged density profiles at several times. There is overall good agreement between our codes for Neptune and Jupiter-sized planets. We performed simulations for each planet in an inviscid disk and including physical viscosity. The surface density profiles agree within about 5% for the grid-based schemes while the particle codes have less resolution in the low density regions and weaker spiral wakes. In Paper II, we study hydrodynamical instabilities in disks with planets. Vortices are generated close to the gap in our numerical models in agreement with the linear modal analysis. The vortices exert strong perturbations on the planet as they move along the gap and can change its migration rate. In addition, disk viscosity can be modified by the presence of vortices.

The second part of this thesis studies the mass transfer in symbiotic binaries and close-in T Tauri binary systems. We study the dynamical effects of gravitational focusing by a binary companion on winds from late-type stars. In particular, we investigate the mass transfer and formation of accretion disks around the secondary in detached systems consisting of an AGB mass-losing star and an accreting companion. The presence of mass outflows is studied as a function of mass loss rate, wind temperature and binary orbital parameters. Our simulations of gravitationally focused wind accretion in symbiotic binaries show the formation of stream flows and enhanced accretion rates onto

the compact component. Mass transfer through wind accretion is an important mechanism for a broad range of symbiotic and wide binary systems and can explain the formation of Barium stars and other chemically peculiar stars. In Paper IV, we study line emission from the accretion flows onto the components of a close young binary system as a function time. We fit the line profiles with four narrow components from the material streaming onto the stars and the circumstellar disks, in qualitative agreement with observations of hydrogen line profiles at some orbital phases.

List of Papers

This thesis is based on the following papers, which are referred to in the text by their Roman numerals.

I de Val-Borro, M., Edgar, R. G., Artymowicz, P., Ciecielag, P., Cresswell, P., D'Angelo, G., Delgado-Donate, E. J., Dirksen, G., Fromang, S., Gawryszczak, A., Klahr, H., Kley, W., Lyra, W., Masset, F., Mellema, G., Nelson, R. P., Paardekooper, S.-J., Peplinski, A., Pierens, A., Plewa, T., Rice, K., Schäfer, C., Speith, R. (2006) A Comparative Study of Disc-Planet Interaction, MNRAS, 370:529-558

II de Val-Borro, M., Artymowicz, P., D'Angelo, G., Peplinski, A. (2007) Vortex Generation in Protoplanetary Disks with an Embedded Giant Planet, A&A, 471:1043-1055

III de Val-Borro, M., Karovska, M., Sasselov, D. (2008) Numerical Simulations of Mass Transfer in Symbiotic Binaries, submitted to ApJ

IV de Val-Borro, M., Gahm, G. F., Stempels H. C., Peplinski, A. (2008) Line Emission from the Close T Tauri Binary V4046 Sgr, submitted to A&A

In Paper I, I did the data analysis and wrote the paper together with R. Edgar. The simulations were run by several groups within the "Planets" EU network, including the planet formation group at Stockholm Observatory. The figures were prepared by me in collaboration with other co-authors.

In Paper II, I carried out part of the numerical work with G. D'Angelo and A. Peplinski, and did the analytical work with P. Artymowicz. The paper and figures were prepared by me together with G. D'Angelo.

I did the numerical simulations and comparison with Bondi-Hoyle accretion theory in Paper III. The paper was written by me together with M. Karovska and D. Sasselov.

In Paper IV, I adapted the FLASH code to study circumbinary disks with A. Peplinski. G. Gahm and H. Stempels helped with the interpretation of the numerical results and comparison with observational data.

Contents

List of Tables

List of Figures

1. Introduction

In this thesis we discuss the results of hydrodynamic simulations of gas disks in binary systems. In Papers I and II, the binary system is formed by a star and a giant planet which is embedded in the circumstellar disk. In Paper III, we consider a symbiotic binary system consisting of a mass losing evolved star and a compact object. A disk forms around the accretor via the gravitationally focused stellar wind. Paper IV studies mass accretion from a circumbinary disk onto a protobinary system on a close orbit.

The last two decades have seen tremendous advances in our understanding of planet formation. In the late 20th century it was recognized that current observational capabilities should be able to discover planets around other stars. The first evidence of planets not belonging to our Solar System came when the first Earth-mass object was discovered unexpectedly orbiting a millisecond pulsar (Wolszczan 1991; Wolszczan & Frail 1992; Wolszczan 1994). This planet is believed to have been formed after a supernova explosion and thus it may have very different properties from the planets in the Solar System. A few years later, the first planet around a main sequence star was discovered (Mayor & Queloz 1995) using high-precision radial velocity measurements. Since then over 300 planets have been found around nearby stars and new discoveries are made regularly (an updated list can be found at the websites of the *Extrasolar Planets Encyclopedia* http://www.exoplanet.eu and the *California & Carnegie Planet Search* http://www.exoplanets.org). New techniques for finding extrasolar planets such as orbital transits and gravitational microlensing are being employed and they can give us more information about the physical characteristics of the planets. It will not be long before we can expect the discovery of the first Earth-mass extrasolar planet.

All of the extrasolar planets discovered so far by means of radial velocity measurements have masses roughly between 0.1 and 11 $M_{♃}$ (where $M_{♃}$ is the mass of Jupiter). Most of these newly discovered systems have orbital properties which do not match those measured in our Solar System. Many extrasolar planets have large orbital eccentricities and orbit their parent star in very tight orbits. These properties were not expected by scientists and have forced a major revision of the theories of planet formation. However, radial velocity measurements have limitations and preferentially detect planets in close orbits, due to the extended observational periods required to detect long-period planets. Terrestrial planets with masses comparable to Earth's mass cannot be observed with current radial velocity techniques.

It has been estimated that around 20% of solar-type stars in the Galaxy may host planets based on results from radial velocity surveys. Systems with multiple planets have been detected from measuring the superpositions of radial velocity variations due to each planet. Only about 20% of the observed planetary systems are known to have multiple planets, although it is likely that many systems with massive planets have smaller yet to be discovered planetary companions.

Planets form from gas and dust particles in thin protoplanetary disks around young stars. The standard model of planet formation consists of three stages which are discussed below. In the first stage, dust particles coagulate or a gravitational instability leads to the formation of kilometer-sized bodies, known as planetesimals. Gravitational interaction between planetesimals in the second stage leads to a runaway growth of the largest body that becomes a planetary embryo. In the third stage, planetary embryos accrete and interact with the remaining gas from the disk. The description of the physical and chemical processes in protoplanetary disks leading to planet formation, and the interaction between the protoplanet and the disk remain a daunting task. Computers are only now becoming fast enough to be able to model these systems in three dimensions including physical mechanisms such as viscosity, magnetic fields and radiation for the long timescales involved in planet formation.

However, beyond the discovery of planets outside the Solar System, the great challenge for astronomers is to find a planet like our Earth which potentially can harbor life. Whether or not life is common in the universe remains yet an unsolved mystery. Developments in observational techniques such as coronography, adaptive optics, and interferometry have taken place in recent years and future space missions like Kepler, Darwin and Terrestrial Planet Finder will be able to detect Earth-like planets in the habitable zone of stars in the vicinity of the Sun. The spatial agencies in the USA and Europe are planning to put those observatories in space within the next decades.

1.1 Outline of the Thesis

In the first part of the thesis, we investigate protoplanetary disks with embedded protoplanets by means of two-dimensional hydrodynamic simulations, with emphasis on the non-linear dynamics of the gravitational interaction between the disk and the forming planets. A wealth of observational data over the last years including observations of extrasolar planetary systems and protoplanetary disks has led to renewed interest in the problem of planet formation and planet-disk interaction. The question whether there are planets around other stars has been asked for thousands of years, however it is only today that our instruments allow us to detect extrasolar planets.

In the second part of the thesis we present simulations of symbiotic binary systems where one of the components is an evolved star with a massive

slow wind that is accreted onto the companion star. In Paper IV, we study a young binary system surrounded by a circumbinary gas disk. We use a shock-capturing code based on FLASH to study the mass transfer in these systems.

The outline of this thesis is as follows. We discuss the history of planet searches and the different methods for detecting extrasolar planets in Chapter 2. Section 2.3 gives a short summary of the orbital properties and correlations of the discovered extrasolar systems. In Chapter 3 we present the current knowledge on planet and star formation and briefly discuss what we have learned about planet formation from observations of extrasolar planetary systems in the last two decades. Chapter 4 summarizes the standard models and evolution of protoplanetary disks where protoplanets are formed. Observations of dust and gas emission from debris disks provide us with important information about the conditions under which protoplanets form and interact with the protoplanetary disk. In Chapter 5 we provide a brief description of analytical and numerical studies of planet migration. Planet migration determines the evolution of planetary systems and may explain why the planets around other stars are different from the planets in our own Solar System. In Chapter 6 we present a review of some of the numerical methods employed to study the problem of planet-disk interactions. Chapter 7 describes wind accreting binary systems. T Tauri binary systems are described in Chapter 8. Finally, we present a short summary of the papers included in this thesis in Chapter 9.

2. Extrasolar Planets

All through history people have speculated about the existence of other worlds similar to ours. The main question has been whether our Earth is unique or there may be other planets harboring life. In ancient Greece, Epicurus and Democritus suggested that there may be other worlds with life around other stars. The Italian philosopher Giordano Bruno asked the same question and suggested that the Sun was only an ordinary star among billions of stars in the sky.

The first physical models of planet formation date back to the 18th century. Planet formation theory had been aimed at explaining our Solar system since Laplace (1796) proposed his standard model for planet formation. This limited view has strongly biased our theories of planet formation until the first extrasolar planet around a main-sequence star was discovered.

Since the beginning of the 20th century, planetary scientists have started to consider the existence of extrasolar planets and the possibility to detect them (see e.g. Spitzer 1939). The first observational attempts to find planets around other stars were performed in the early 20th century using the astrometric method (Strand 1943). van de Kamp (1963) announced the detection of a planet with a mass of about 1.6 Jupiter masses on a 24-year orbit around Barnard's star, which is the star with the largest proper motion in the sky. Unfortunately, none of these early detections withstood the test of time. It is still not clear if Barnard's star really has a planet due to the difficulty in observing the star for one full period of the planet. After several false detections (van de Kamp 1982; Bailes et al. 1991) a planet was found orbiting the main sequence star 51 Peg at 0.05 astronomical units (AU) (Mayor & Queloz 1995). Since 1995, more than 300 planets have been discovered orbiting stars other than the Sun.

More than twenty planets have been detected every year during the last few years, with the discovery rate increasing drastically since 2007. Most of these objects have been discovered or confirmed measuring the radial velocity of the parent stars. It has been estimated that at least 7% of solar-type stars have a giant planet within 5AU (Marcy et al. 2005) but the percentage of stars hosting planets at larger distances may be much higher. Microlensing surveys suggest that nearly 45% of M dwarfs in the Galactic bulge have a giant planet at $1-4$ AU from its host star. The discovery of extrasolar planets gives new focus to the question of whether some systems might support life.

Most of the newly discovered planets have masses which are about the same or larger than Jupiter's. It is not known if the planets would resemble the gas giants in our solar system or if they have a completely different composition. Extrasolar planets which orbit extremely close to their parent stars receive much more stellar radiation than the gas giants in our solar system. It is possible that their atmospheres are being blown away by their host star radiation. Neptune-mass planets have been detected that may have been formed from 'Hot Jupiters' via evaporation (Baraffe et al. 2004).

Planets do not produce light by means of nuclear fusion and therefore are extremely faint light sources compared to their parent stars. In addition to the intrinsic difficulty of detecting such a faint light source, the distance from the observer to the planet is much larger than the distance from the planet to its star, which generates a glare that wipes out the signal from the planet. Thus, the photons emitted by the planet cannot be detected with current instrumentation and astronomers use indirect methods to find exoplanets.

2.1 Observational techniques

In order to understand how terrestrial and giant planet forms it is necessary to consider the properties of the discovered extrasolar planetary systems.

Light contrast ratios of 10^{10} (at visible wavelengths) to 10^{7} (in the infrared) between a star and planet make direct detection by imaging extremely hard. However, mass ratios are of the order $10^{3} - 10^{5}$ which allows the detection of the reflex motion of the star from the gravitational pull of the planet.

2.1.1 Radial velocity technique

The most successful way of spotting extrasolar planets is through its gravitational pull on its parent star. The radial-velocity or Doppler method uses the fact that a planet-bearing star moves in its own small orbit in response to the planet's gravity. This is measured through the displacement in the star's spectral lines, which is proportional to the mass ratio, and the radial velocity along the line of sight can be deduced. A Keplerian fit to the data points gives an estimate of the period and other orbital parameters such as semimajor axis, eccentricity, inclination, longitude of pericenter and time of pericenter (Marcy & Butler 1998).

This technique to detect planets was first proposed by Struve (1952). Astronomers are able to measure variations in the radial velocity of the star with errors of less than 1 $\mathrm{m\,s^{-1}}$with current instruments (Pepe et al. 2004). The radial-velocity technique is now responsible for the discovery of about 90% of the known exoplanets.

The semi-amplitude of the stellar radial velocity induced by a planetary companion is

$$K = v_* \sin(i) = \left(\frac{2\pi G}{P_s}\right)^{1/3} \frac{M_\mathrm{p} \sin i}{(M_* + M_\mathrm{p})^{2/3}} (1 - e_s^2)^{-1/2}, \tag{2.1}$$

in which M_* is the stellar mass, M_p the planetary mass, P the orbital period, e the eccentricity and i the inclination.

Assuming that $M_* \gg M_p$ the semimajor axis can be obtained as

$$a = \left[\frac{G(M_* + M_\mathrm{p})P^2}{4\pi^2}\right]^{1/3}. \tag{2.2}$$

Short period planets are easier to detect with these technique since less observational time is required and the gravitational pull on their host star is larger. Velocity variations smaller than 1 $\mathrm{m\,s^{-1}}$can be discerned with modern instrumentation such as the High Accuracy Radial Velocity Planet Searcher (HARPS) spectrometer at European Southern Observatory, or the High Resolution Echelle Spectrometer (HIRES) at the Keck telescopes.

High signal-to-noise ratios are required to achieve high precision and therefore this method is generally only used for relatively nearby stars out to about 150 light-years from Earth. This technique allows for the determination of the planet's minimum mass due to the uncertainty in the orientation of the planet's orbit with respect to the line of sight. The real mass of the planet can be determined combining radial velocity observations with very precise astrometric measurements of the movement of the star in the sky using future space telescopes.

2.1.2 Transiting planets

Extrasolar planets can be detected by means of the characteristic photometric signature on the star caused by an eclipsing planet. A Jupiter-sized planet crossing in front of its star's disk causes a drop in the stellar brightness by an amount of the order of 1%, while a terrestrial planet obscures about 0.01% of the stellar luminosity. The fractional dimming f during the transit can be used to obtain important properties of the planet:

$$f = \frac{\Delta L_*}{L_*} = \left(\frac{R_\mathrm{p}}{R_*}\right)^2, \tag{2.3}$$

where R_p/R_* is the planet-star radius ratio and L_* is the stellar luminosity.

The parameters of greatest interest are the inclination and the planet's radius, which may be estimated for certain assumptions (Seager & Mallén-Ornelas 2003). Obtaining the inclination will remove the mass degeneracy and the radius will allow one to estimate the planet's density. Transit photometry and eclipse timing have become today the second most productive planet detecting technique.

Transit observations combined with radial velocity measurements allows us to determine the bulk density of the planet and learn something about its physical characteristics. Planetary transits are only observable for the small percentage of planets whose orbits happen to be aligned with our line of sight and therefore only ~ 50 objects have been detected with both methods so far. Most of these planets have low densities and must be made up of hydrogen and helium like the giant planets in the solar system.

The transit method also allows to study the atmosphere of the transiting planet. When the planet crosses the star's disk, light from the star is filtered through the atmosphere of the planet. The elements present in the planet's atmosphere can be detected in the stellar spectrum allowing astronomers to study the chemical composition and temperature of the atmosphere (Charbonneau et al. 2002).

A new technique to detect Earth-mass Trojans using radial velocity and transit observations has been proposed by Ford & Gaudi (2006). Trojan satellites are located at the Lagrangian points L_4 or L_5, sharing the same orbit and separated 60° from the planet. The existence of Trojans of the transiting planets in the systems HD 209458 and HD 149026 has been ruled out. Transit timing observations can also be used to detect Trojans of transiting extrasolar planets (Ford & Holman 2007).

2.1.3 Astrometry

Astrometry is the oldest search method for extrasolar planets, used as early as 1943, and has been unsuccessful to date but it has been used to confirm several exoplanets. A star's position in the sky can be measured accurately and by observing how that position changes over time it is possible to detect the presence of a planet. If the star has a planet the gravitational influence of the planet will cause the star itself to move in an elliptical orbit whose angular semimajor axis is

$$\alpha = \frac{M_\mathrm{p}}{M_*}\frac{a}{d}, \tag{2.4}$$

where a is the semimajor axis and d is the distance from the Earth to the host star. Star and planet orbit around the barycenter as explained by solutions to the two-body problem. Astrometry is able to detect small planets at large distance from its host star, although very long observation times are needed. More details on how efficient astrometry is for finding various types of planets has been calculated by Ford (2004).

Since this method is sensitive to long orbital periods and can be used for hot and pulsating stars, astrometric measurements are complementary to Doppler observations. Astrometric observations can constrain the system inclination which allows for the mass determination. Furthermore, the relative inclination of the planets in multi-planet systems sets strong constraints on the dynamical evolution of the system.

2.1.4 Microlensing

Gravitational microlensing occurs when the gravitational field of a foreground object acts like a lens, magnifying the light of a distant background star. This effect was first considered by Einstein in 1936. Microlensing occurs only when the two stars are almost exactly aligned. Lensing events are brief, lasting for weeks or days, as the two stars and Earth are all moving relative to each other.

If the foreground lensing star has a planet, then that planet's own gravitational field can make a detectable contribution to the lensing effect. The presence of a Earth-sized planet at several AU from the foreground star can be detected with this method, which makes gravitational microlensing the only technique currently able of detecting terrestrial planets around main-sequence stars. Since that requires a highly improbable alignment, a very large number of distant stars must be continuously monitored in order to detect planetary microlensing contributions at a reasonable rate. This strategy is most fruitful for planets between the Earth and the center of the galaxy, as the galactic center provides a large number of background stars. There are currently 7 exoplanets detected by this technique. The first low-mass planet on a wide orbit, designated as OGLE-2005-BLG-390Lb, was discovered by gravitational microlensing (Beaulieu et al. 2006).

2.1.5 Pulsar planets

The first firm discovery of planetary objects came completely unexpected as Earth-sized planets were found orbiting a burned-out stellar remnant, the pulsar PSR B1257+12 (Wolszczan & Frail 1992). The extremely stable rotation of pulsars provides a high-precision clock, which can be used for the indirect detection of planets, in a way that is quite similar to the radial-velocity method discussed in Section 2.1.1. High-precision monitoring of the time-of-arrival of the radio pulses can reveal subtle motions of the pulsar, such as its reflex motion due to the presence of a planetary companion. The amplitude of timing residuals for a planet on a circular orbit with mass $M_{\rm p}$ is given by

$$\tau = 1.2\text{ms} \left(\frac{M_{\rm p}}{M_\oplus} \right) \left(\frac{P}{1\text{yr}} \right)^{2/3} \sin(i), \tag{2.5}$$

where P is the period, i represents the inclination and a neutron star mass of $1.35 M_\odot$ is assumed.

2.1.6 Direct Detection

To directly image an exoplanet is difficult because of the large luminosity difference between the star and the planet. Current instruments are only starting to become good enough to detect the small fluxes emitted by the planets in close proximity to their stars (Beuzit et al. 2007).

Most exoplanets have been discovered through radial velocity measurements and transit photometry. However, the imaging detection of a young Jupiter around a nearby star is within the reach of current adaptive optics instruments on $8-10$ meter telescopes but no detections have been made so far. Young giant planets are hot and bright, making them significantly easier to detect through near-infrared imaging than their older counterparts. With the commission of new instruments in the infra-red and ground-based interferometers, it may also be possible to detect older giant planets around nearby main sequence stars, particularly with the use of the so-called nulling interferometry technique to block out the light of the star.

2.1.7 Future searches

Most of the extrasolar planets that have been discovered so far are giants like Jupiter and Saturn. They are unlikely to support life as we know it. But some of these planetary systems might also contain smaller, terrestrial planets like Mars and Earth where temperatures would be suitable for liquid water to exist. It has been proposed that exoplanets may have habitable satellites (Scharf 2006; Cabrera & Schneider 2007). Habitable zones move out as stars evolve and for solar type stars the duration may be long enough for life to evolve.

The Space Agencies of the United States and Europe have programs underway to develop a Terrestrial Planet Finder satellite, which would be capable of imaging planets with masses comparable to terrestrial planets. NASA's Kepler Space Observatory, set to launch in 2009, will make use of the transit method to detect Earth-mass planets.

During the next years we will know if extrasolar Earth-like planets are different from the objects in our solar system and how frequent they are in astronomical terms. The discoveries of giant planets orbiting unexpectedly close to their host stars suggests that there may be more surprises and exciting results in the future. We will also have the possibility to test the current planet formation theories and expand our understanding of the processes that lead to planet formation.

2.2 Solar System Planets

The properties of the planets in the Solar System are listed in Table 2.1. The planets in the Solar System orbit the Sun in a plane that is roughly perpendicular to the Solar rotation and have low relative inclinations. All the planets and most minor objects orbit in the Sun's rotation direction. The Solar System is composed of four inner terrestrial planets, the asteroid belt, four giant planets, the Kuiper belt and the Oort cloud. The terrestrial planets are composed of silicates and metals. There are two large terrestrial planets (Earth and Venus) and two smaller ones (Mercury and Mars). The three outer terrestrial

Table 2.1: *Orbital parameters and masses of the planets in the Solar System from Armitage (2007).*

	a (AU)	e	$M_{\rm p}$ (g)
Mercury	0.387	0.206	3.3×10^{26}
Venus	0.723	0.007	4.9×10^{27}
Earth	1.000	0.017	6.0×10^{27}
Mars	1.524	0.093	6.4×10^{26}
Jupiter	5.203	0.048	1.9×10^{30}
Saturn	9.537	0.054	5.7×10^{29}
Uranus	19.189	0.047	8.7×10^{28}
Neptune	30.070	0.009	1.0×10^{29}

planets have significant atmospheres. The two gas giants (Jupiter and Saturn) are composed mainly of hydrogen and helium, while the smaller ice giants (Uranus an Neptune) have a core composed of water, ammonia and metals and an atmosphere composed of hydrogen and helium. All the planets in the Solar System have low eccentricities except for Mercury.

The Titius-Bode law states that the distances d of the planets to the Sun are given by

$$d = 0.4 + 0.3 \times 2^i, \tag{2.6}$$

where $i = -\inf, 0, 1, 2, 4, 5, \ldots$. This law fits surprisingly well the position of the planets despite its lack of a physical basis. However, Murray & Dermott (2000) have shown that almost any planet distribution can have its own Titius-Bode law.

Most of the mass of the system, including metals, is contained in the Sun, but the total angular momentum is dominated by the orbital angular momentum. It is usually assumed in planet formation models that the surface density profile in the primordial nebula has the dependence

$$\Sigma = 10^3 \left(\frac{r}{\rm AU}\right)^{-3/2} {\rm g\,cm^{-2}}. \tag{2.7}$$

This profile is reconstructed from the mass of the current planets increased with lighter elements to reach solar composition. The solar nebula had a high metallicity content enriched by elements formed in previous stellar generations. This has been crucial to allow the formation of a planetary system according to planet formation theories.

2.2.1 Minor Bodies

The asteroid belt is a reservoir of minor bodies in the Solar System between the orbits of Mars and Jupiter. It contains bodies of rocky and metallic compo-

sition up to a few 100 km in diameter at a distance between $2.3-3.3$ AU from the Sun. It is believed that gravitational perturbations from Jupiter prevented the planetesimals in the asteroid belt to form a planet. In addition, Jupiter has an asteroid family located at the L_4 and L_5 Lagrangian equilibrium points, the so-called Trojan asteroids, which is not considered part of the asteroid belt.

The trans-Neptunian region consist of small bodies in the Kuiper belt and scattered disk which is the origin of short-period comets (Chiang et al. 2007). The Kuiper belt is a ring of objects between $30-50$ AU composed primarily of ice. There are two known dwarf planets in the Kuiper belt, Pluto and Eris.

2.3 Statistics of Extrasolar Planetary Systems

More than 300 planets have been detected which allows for the first statistical studies to be performed. The properties of observed planetary systems are very different from what scientists originally expected. Many of the detected planets are giant gaseous bodies with a period of only a few days. Some of the planets orbit their stars on very eccentric orbits compared with their counterparts in the Solar System. However, the Doppler technique has a strong bias in favor of massive planets in short-period orbits and it is not yet clear whether the Solar System is a unique system. Current instruments are able to detect wobbles of less than $K \sim 1\mathrm{m\,s^{-1}}$ (this limit is shown in Fig. 2.2). Most of the currently available extrasolar planetary data such as minimum mass, semi-major axis and eccentricity are derived from Doppler observations. All the data presented in this chapter have been retrieved from the *Extrasolar Planets Encyclopedia* [1] compiled by Jean Schneider.

The distribution of planets in $M_\mathrm{p}\sin(i)$, a, and e are shown in Figures 2.1, 2.2 and 2.3. In Fig. 2.2 the minimum mass is plotted as a function of the semi-major axis in logarithmic scale. There seems to be a scarcity of planets at distances ~ 0.3AU and a pile-up at short distances ~ 0.05AU. It is not expected that planets could form at such a short distance from the star and therefore orbital migration due to interaction with the gaseous disk seems a likely mechanism to bring the planets to close distances.

A power law has typically been used to describe the mass distribution of exoplanets (see Fig. 2.4). Recent work has shown that a broken power law provides a better fit to the data Butler et al. (2006).

$$dN/dM \propto \begin{cases} M^{-1.2} & M < 0.6 M_{♃} \\ M^{-1.9} & M > 0.6 M_{♃} \end{cases} \tag{2.8}$$

It is not possible to extrapolate the mass distribution to lower masses since the formation mechanisms for Earth-sized planets may be different.

[1] http://www.exoplanet.eu

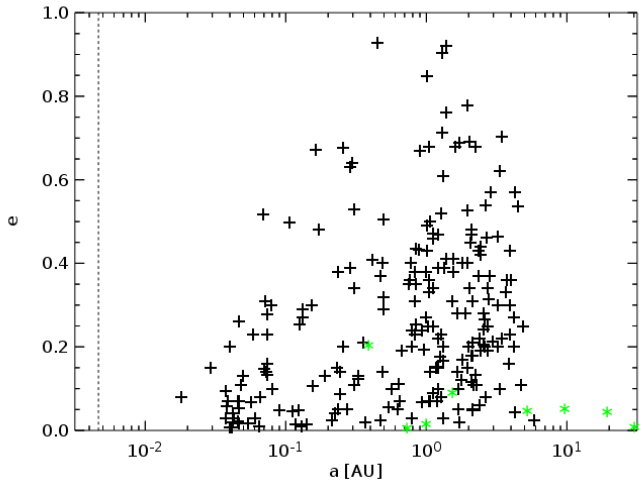

Figure 2.1: Diagram of the eccentricity versus semimajor axis in logarithmic scale. Planets in the solar system are represented by green dots. The dashed vertical line indicates the position of the solar surface.

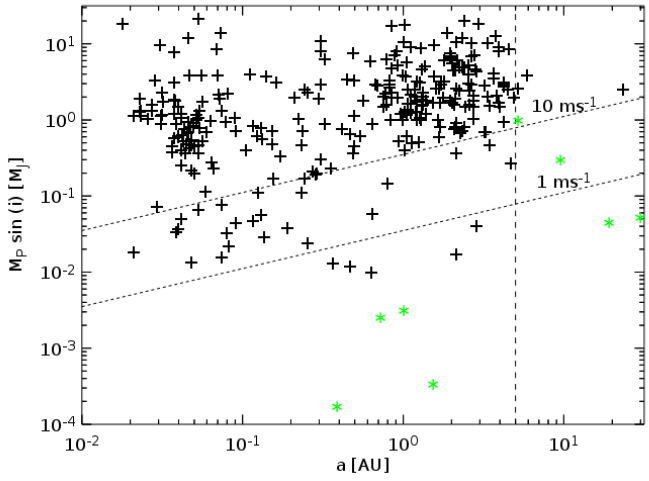

Figure 2.2: Minimum mass versus orbital semimajor axis for extrasolar planet candidates in logarithmic scale. The dotted lines represent the detection limit of the radial-velocity method for velocity amplitudes of $10\,\mathrm{ms}^{-1}$ and $10\,\mathrm{ms}^{-1}$ assuming a solar mass host star. The vertical dashed line shows the selection limit of current surveys. Green dots represent the mass of solar system planets.

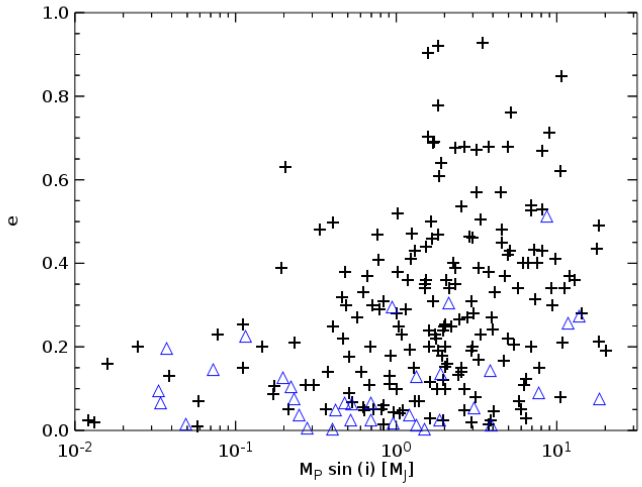

Figure 2.3: Eccentricity versus planet mass for extrasolar planets. Short period planets with periods < 10 days are shown with blue triangles, while long period planets with periods > 10 days are denoted with black crosses.

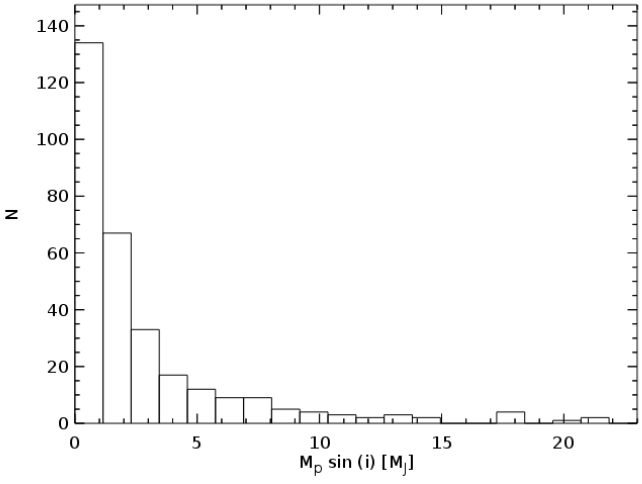

Figure 2.4: Planetary mass function in linear scale.

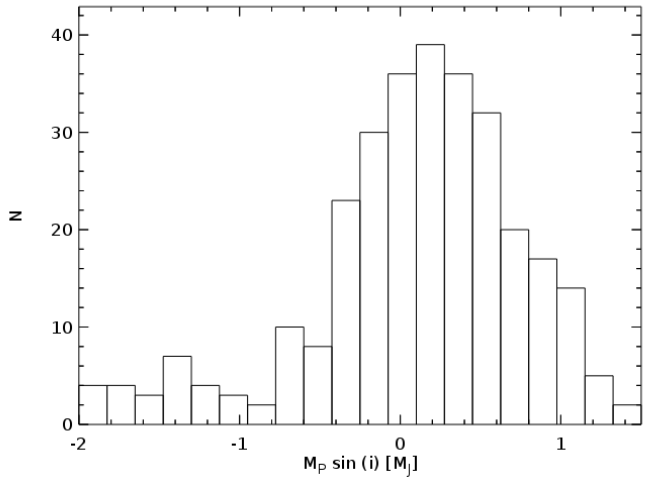

Figure 2.5: Planetary mass histogram in logarithmic scale.

Fig. 2.5 shows the histogram of the lower limit on the mass $M_{\rm p}\sin(i)$ for extrasolar planets in logarithmic scale. There is a remarkable dearth of planets with minimum mass above $10M_{♃}$ which has been referred to as the brown dwarf desert. Most of the detected planets are in the range $0.5-3M_{♃}$ (Butler et al. 2006). Since Doppler surveys preferentially detect massive planets, we can conclude that there is a shortage of massive planets in very close orbits.

Fig. 2.1 shows the orbital eccentricity versus semi-major axis for extrasolar planets and Solar System planets marked by green dots. The orbits of close planets with semi-major axis less than ~ 0.05 AU have small eccentricities. This has been explained by tidal dissipation of energy within the planetary envelopes (Rasio & Ford 1996). Eccentric orbits are common beyond the tidal circularization radius with median value $<e>\sim 0.25$. A few planets have very high eccentricities ~ 0.9. In Fig. 2.3 eccentricity is plotted versus projected planet mass, with short period planets denoted by blue triangles. There is no apparent correlation between eccentricity and mass.

Multiple planet systems are common, and about a third of them are in mean-motion resonance.

2.4 Metallicity Enhancement

The chemical composition observed from the star reflects the abundance of raw materials, including heavy elements, available in the disk to build planets. The observational data are consistent with the hypothesis that heavier elements stick together easier, allowing dust, rocks and eventually planetary

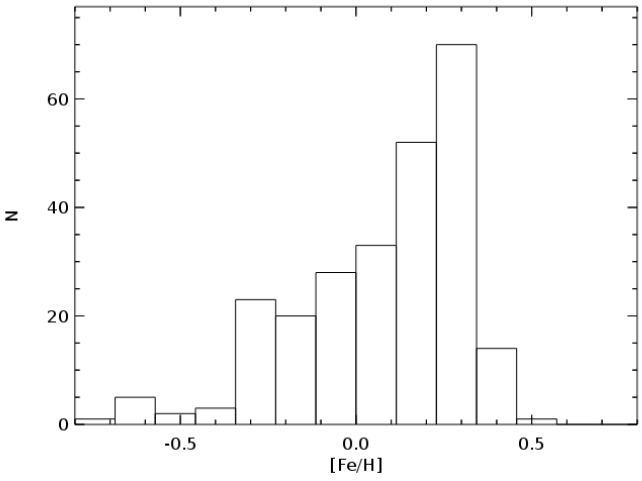

Figure 2.6: Metallicity distribution [Fe/H] of planet hosting stars.

cores to form in metal rich disks. Planets are more often found around more metal rich stars as predicted by the core accretion model, since a higher density of solid grains should make planet formation easier. The probability of finding a planet increases rapidly for stars with higher iron abundance (Butler et al. 2006).

The distribution of stars hosting planets as a function of stellar metallicity [Fe/H] is presented in Fig. 2.6. Most planets have been found in stars which are significantly more metal rich than the Sun. However, there is a slight observational bias towards detecting planets in metal-rich stars. Radial velocity surveys detect preferably planets in high metallicity stars that have deep absorption lines. Moreover, Doppler survey samples may be enriched with metal-rich stars since they are brighter than metal-poor stars. Despite those biases, a number of studies have shown that the correlation between metallicity and presence of planets is real (see e.g. Santos et al. 2003).

Iron and other heavy-element atoms are formed in the interior of stars by nuclear fusion and thrown into the interstellar medium by supernova explosions. They were extremely rare in the early Universe and each successive generation of stars has a greater abundance of heavy elements. Thus, stars forming today are more likely to harbor planets than earlier generations of stars. It is expected that the protoplanetary disk should have the same composition as the star and therefore this observed correlation is consistent with the core accretion scenario discussed below, where dust particles stick together and finally form planetary embryos that can accrete gas from the disk.

2.5 Search for Extraterrestrial Intelligence

The discovery of extrasolar planets has renewed interest in the possibility of life and intelligent civilizations in planets outside our Solar System. There have been numerous speculations about the presence of life elsewhere in the Universe (Dick 1982). Other planets in the Solar System are thought not to be inhabitable, although some authors have considered life on Venus (e.g. Schulze-Makuch & Irwin 2002).

The search for extra-terrestrial intelligence (SETI) project was funded initially by NASA in 1971 to search from radio signals from other civilizations in our Galaxy. The number of civilizations that may be able to communicate over interstellar distances has been estimated using the Drake equation (Drake 1962). The number of communicating civilizations in the Galaxy, N, is given by the formula

$$N = R_* \times f_p \times n_h \times f_l \times f_i \times f_c \times L, \tag{2.9}$$

where R_* denotes the rate of star formation in the Galaxy in stars per year, f_p is the fraction of stars with planetary systems, n_h is the average number of planets with with favorable conditions for life to develop, f_l is the fraction of habitable planets on which life actually appears, f_i is the probability that evolution generates intelligent life, f_c is the fraction of intelligent civilizations that attempt to communicate over interstellar distances and L is the length of the communication phase in years. The factors in the Drake equation are highly uncertain and have been disputed over the years. However, it may be possible to determine observationally f_p and n_h over the next decades with good accuracy. Drake (1962) estimated that $N \sim 10$ although different assumptions can give values of $N \ll 1$.

3. Theory of Star and Planet Formation

This chapter reviews the theory of star and planet formation. The subject of planet formation has undergone a large growth in the last 15 years with the discovery of the first planets orbiting nearby stars and detailed observations of protoplanetary disks. Before the discovery of extrasolar systems the planetary scientists concentrated on describing the properties of our Solar System in great detail. The detection of extrasolar planetary systems has revealed an unexpected diversity of planetary systems that has revolutionized planet formation theory.

According to current observations, at least 12% of stars of spectral type F, G, K harbor gas-giant exoplanets on orbits smaller than 20 AU (Marcy et al. 2005), showing that planet formation is a common process. The standard planet formation model was proposed by Safronov (1969), where protoplanets form in gaseous disks around young stars due to the collisions of dust grains followed by solid body accretion (for recent reviews on planet formation see e.g. Lissauer 1993; Papaloizou & Terquem 2006). Therefore, the origin of planetary systems is closely coupled to the formation of their host stars. The core accretion theory that explains the formation of gaseous giant planets from protoplanets was laid out by Mizuno (1980). An alternative scenario for the formation of giant gaseous planets is the so-called core collapse model (Boss 2001). This model is related to the original model of Kant and Laplace, where giant planets form through fragmentation and gravitational collapse in the outer regions of protoplanetary disks.

3.1 Star Formation

In this section we summarize aspects of star formation that are relevant for planet formation theory. In particular, we focus on low-mass star formation. Excellent reviews of star formation can be found in Shu et al. (1987); Hartmann (1998); McKee & Ostriker (2007).

Stars form in the Galaxy from the gas in dense clouds consisting mainly of molecular hydrogen. Molecular clouds typically have a clumpy structure and stars are formed in the dense regions. The main four stages of star formation are shown in Fig. 3.1. In the first stage of star formation, turbulent processes within the molecular cloud lead to dense regions reaching a critical density

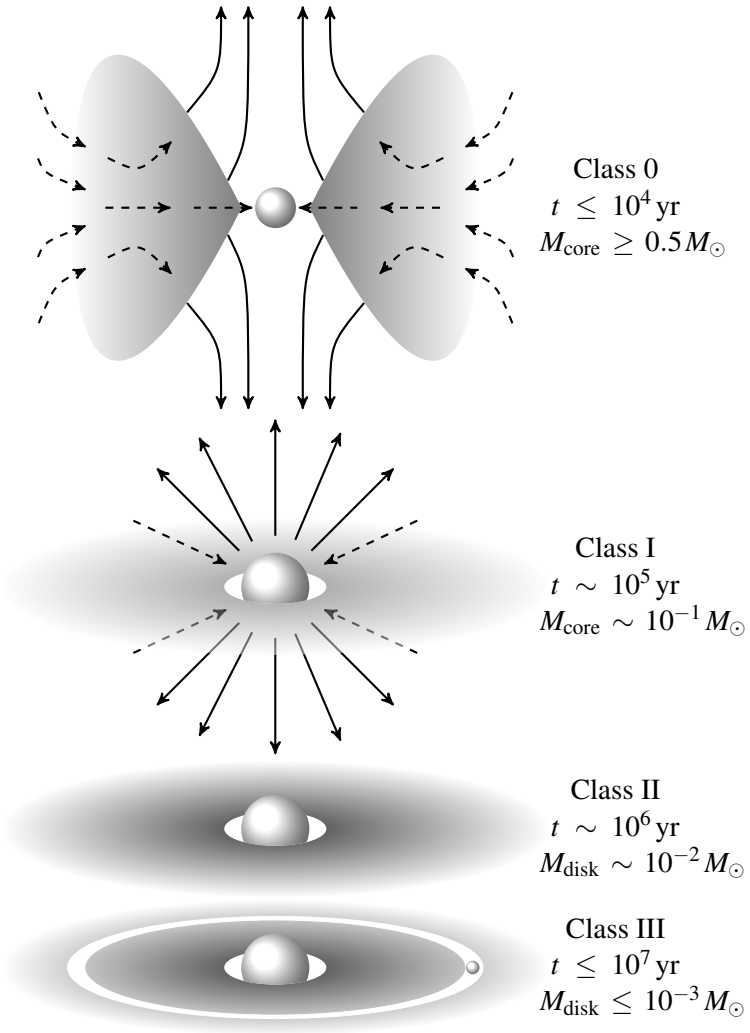

Figure 3.1: Stages of low mass star formation according to André (1994).

such that a clump collapses under its own gravity. Observations of the clouds cores in molecular tracers such as CO, ^{13}CO and NH_3 can be used to constrain column density and to provide information on accretion and outflows. The rotation energy of the dense cores can be characterized by the ratio of the rotational energy to the gravitational binding energy

$$\beta_{\mathrm{rot}} \equiv \frac{E_{\mathrm{rot}}}{|E_{\mathrm{grav}}|} \tag{3.1}$$

This parameter is small for a uniformly rotating sphere, $\beta_{\mathrm{rot}} \sim 0.03$. Therefore, rotation is dynamically unimportant during the gravitational collapse phase. The angular momentum is in the range $j \sim 10^{54} - 10^{56}\,\mathrm{g\,cm^2 s^{-1}}$, and is much larger than the angular momentum in the Solar System.

In the so-called core collapse stage, dense regions of molecular clouds with densities greater than 10 cm^{-3} gravitationally collapse. This stage lasts for about $10^4 - 10^5$ years and is an almost isothermal gravitational self-contraction of the cloud core. Cores above a critical mass will start gravitational fragmentation. The minimum wavelength for self-contraction was calculated by Jeans (1902) assuming that the only force opposing gravity is the thermal pressure.

$$\lambda_J = \left(\frac{\pi \sigma_{th}^2}{G \rho_0} \right)^{1/2}, \tag{3.2}$$

where σ_{th} is the thermal speed and ρ_0 is the density of the cloud. According to the Jeans criterion, a cloud core of gas with temperature T, density ρ_0, and mean molecular mass μ will self-contract under its own gravity if its mass is above the Jeans critical mass.

The gravitational energy from the infall is radiated away. As the density of the collapsing core increases, the efficiency of the radiative release decreases and the collapse stops due to the build up of thermal pressure. Due to the conservation of angular momentum, the rotation increases as the cloud collapses and causes the gas to flatten out forming a protoplanetary disk. The detailed structure of disks can be inferred from spectroscopy and spectral energy distributions (SEDs).

During the third stage, the so-called protostellar phase, the dense core is subject to a quasi-static contraction and the protostar accretes most of the remaining mass (Larson 2003). The protostellar core becomes hot enough to start nuclear fusion of deuterium and slowly contracts in quasi-hydrostatic equilibrium. After that time the star reaches a surface temperature similar to that of a main sequence star of the same mass and becomes visible since the envelope is optically thin. Most of the core material will have sufficient angular momentum to form a rotating accretion disk around the protostar. The duration of the protostellar phase is typically $10^5 - 10^6$ years for solar-type stars. It is believed that bi-polar outflows during the protostellar stage can remove angular momentum efficiently from the system.

In the fourth stage, the envelope is dispersed due to a combination of accretion onto the star and strong bipolar outflows. The remaining star is called a T Tauri star and has a surrounding thin disk where planets are formed. The gas disk is dispersed due to accretion and photoevaporation within about 10^7 years. When most of the material in the disk is blown away or accreted a gas-poor disk remains consisting of dust and small rocks. Once a protostar starts to burn hydrogen, it becomes a main sequence star, a phase that lasts for a few 10^9 years.

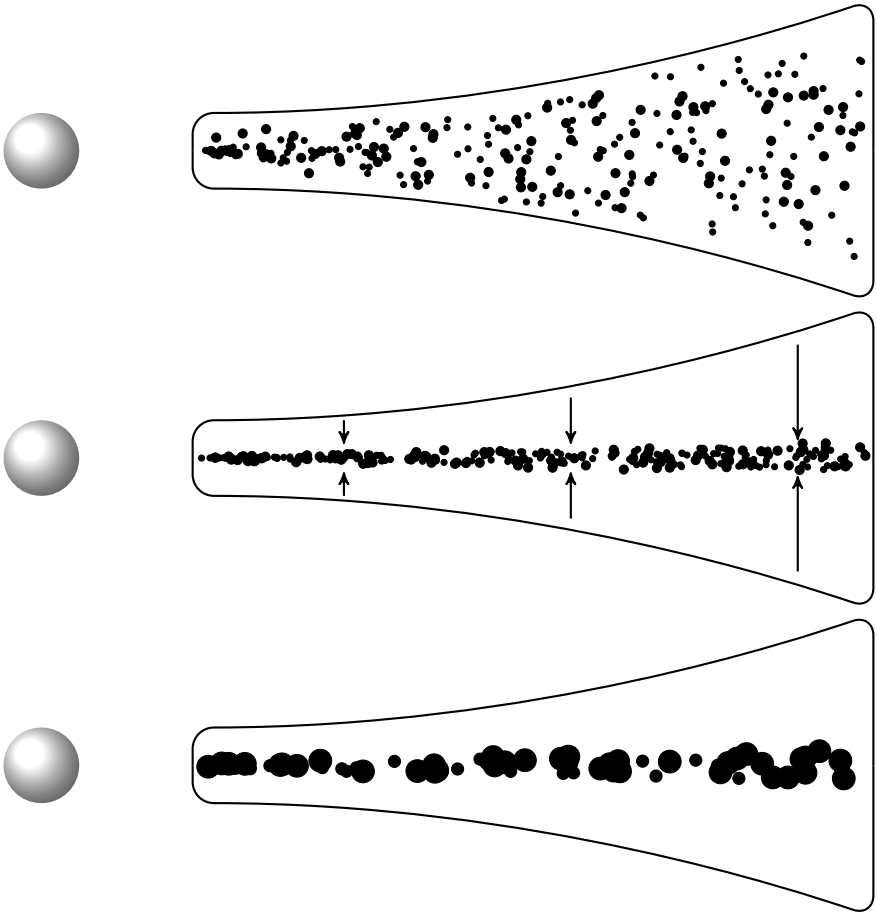

Figure 3.2: Illustration of the Goldreich-Ward scenario (Goldreich & Ward 1973). Dust particles form a dense layer in the midplane that can lead to a gravitational instability.

3.2 Terrestrial Planet Formation

Planets are believed to be a byproduct of the star formation process. The theoretical study of planet formation has a long history. Some of the main ideas in the theory of terrestrial planet formation were first introduced in the late 1960's by Safronov (1969). Planets are formed in rotating disks of gas and dust surrounding newly formed stars. These disks have radii up to a few thousands AUs and rather cool temperatures of a few hundred Kelvins.

Terrestrial planets are formed from planetesimals by accretion of solid particles. Planetesimals are kilometer-sized bodies formed from collisional growth and coagulation of dust grains. The formation of planetesimals is still a poorly understood area. Observations indicate that planetesimals form on a short time scale compared with the life of the disk. Goldreich & Ward (1973) suggested that due to gravitational settling and radial drift, dust forms a dense midplane

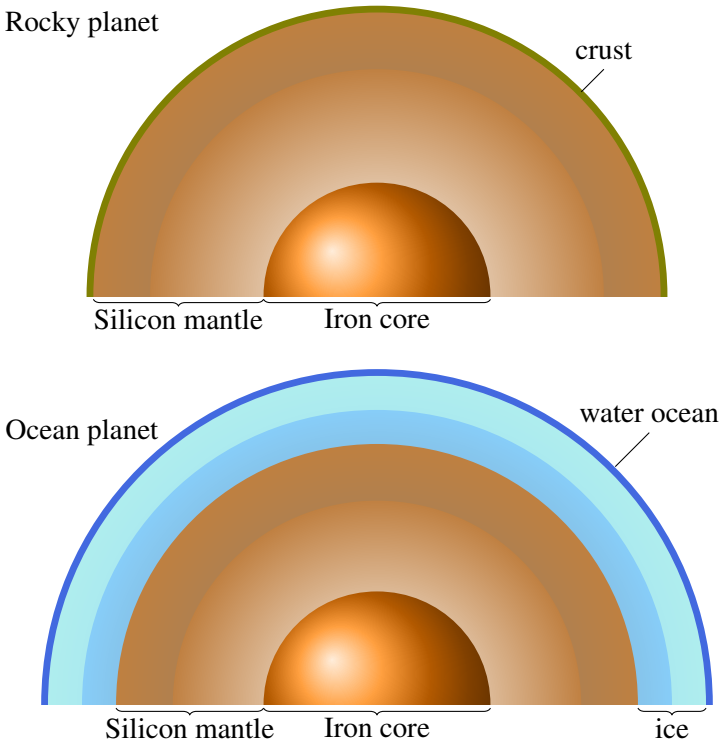

Figure 3.3: Composition of Super-Earth rocky and ocean planets.

layer that becomes gravitationally unstable. Fig. 3.2 shows a sketch of the Goldreich-Ward mechanism leading to formation of planetesimals. However, the disk needs to be sufficiently massive to develop a gravitational instability and turbulence in the disk may prevent the formation of a thin dust layer. For a recent review of dust growth see Dominik et al. (2007).

Planetesimals collide and accumulate due to mutual gravitational interaction to form larger bodies. Further growth takes place as planetary embryos accrete solid bodies and gas once they reach a size $> 10^3$ km. Fig. 3.3 illustrates the composition of rocky and ocean super-earths, planets with masses in the range 1 to 10 Earth masses. The planets originally are composed of a mixture of water, ammonia and solids. Iron and heavy elements form a core. If there is a substantial amount of water, an ocean mostly composed of ice water due to high pressures will be formed over the silicate mantle. Theoretical models show that an accuracy of 5% in radius determination and 10% in mass are needed to differentiate between the two types.

These planetary cores can grow in mass surrounded by a quasi-static gaseous atmosphere until they reach a critical mass and rapid gas accretion leads to the formation of giant planets.

3.3 Giant Planet Formation

The prevailing theory is that giant planets are formed in a two-step process. In the first step, electrostatic and gravitational forces cause the dust and ice grains in the disk to accrete into solid planetesimals which collide and clump together to form a protoplanetary core. The core becomes eventually massive enough to gravitationally attract a massive gaseous envelope from the surrounding nebula (Pollack et al. 1996). This is known as the core accretion model for giant planet building. Initially, the envelope remains in quasistatic equilibrium radiating energy supplied by the accretion of planetesimals. When the core reaches a critical value of a few Earth masses, the envelope starts to contract and accrete gas very rapidly. This process goes on for about 10 million years, until the remaining material falls onto the star or is dispersed by the young star's wind as inferred from observations of protoplanetary disks around young solar-type stars.

According to the disk instability model, planets are formed directly from blobs in the primordial disk that collapse by their own gravity to form protoplanets. This is a very rapid process that can create a Jupiter mass planet in a few thousand years. Numerical simulations have shown that Jupiter-mass objects can form at several AUs from the star in eccentric orbits. This model has difficulties explaining the presence of large cores and heavy elements in the atmosphere of the giant planets in the solar system. It is possible that both planet formation mechanisms could occur under different situations.

Both theories are currently being studied. As the number of discovered planets increases, the formation models will be tested and statistical studies of planetary systems will allow us to advance our understanding of the physical and chemical processes involved in planet formation.

4. Circumstellar Disks

This chapter reviews the topic of protoplanetary disks and their evolution to understand what are the conditions in disks around young stars during planet formation. The detailed structure and evolution of protoplanetary disks is not yet completely understood but we have learned a lot about disk structure and dynamics from recent observations of dust and gas emission. Unfortunately, the initial stages where planets form from planetesimals cannot be observed directly.

4.1 Disk Evolution

Disks around young stellar objects (YSOs) are detected by their near-infrared flux excess. Dust particles close to the star heat up when they absorb stellar radiation and reradiate in the thermal infrared. Protoplanetary disks are classified observationally into four different classes according to their slope in the near-infrared $\alpha_{\rm IR} = \Delta\log(\lambda F_\lambda)/\Delta\log\lambda$.

Passive disks are not powered by accretion and release mostly reprocessed radiation from the central star. On the other hand, radiation from active disks is dominated by the release of gravitational energy. Passive disks around pre-main sequence stars are relatively massive ($\sim 0.01 M_\odot$) and usually present a flaring geometry, where the scale-height increases with radial distance from the star (Kenyon & Hartmann 1987). The vertical structure of a geometrically thin disk can be calculated using the vertical hydrostatic equilibrium condition

$$\frac{{\rm d}P}{{\rm d}z} = -\rho g_z \tag{4.1}$$

where ρ is the gas density.

The gaseous disk is dispersed due to accretion onto the star and photoevaporation by the ionizing UV radiation (see Fig. 4.1). Initially, radiation heats the surface of the disk to temperatures $\sim 10^4$ K that creates an extended atmosphere above the midplane and an inner gap forms in the inner disk. A wind of about 10 km s^{-1} blows away the outer parts of the disk. When the inward viscous drain is compensated by the outward flow due to photoevaporation at the critical radius r_g, the disk is no longer resupplied and is cleared on a short timescale. The dispersal timescale for disks around solar-mass stars is typically $\sim 6\times 10^6$ years (Alexander et al. 2006). This is an important constraint for models of planet formation.

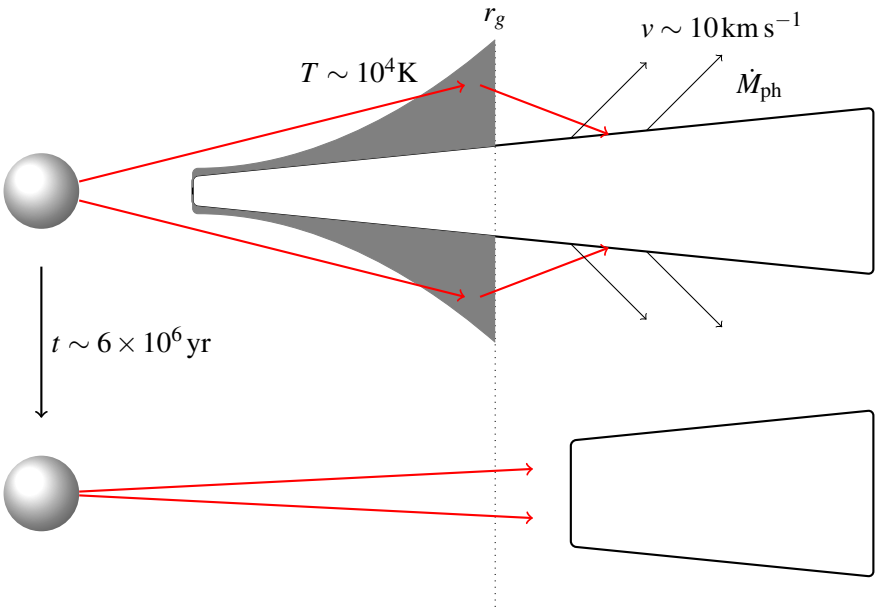

Figure 4.1: Illustration of disk dispersal by UV radiation from a central star. The red arrows represent UV radiation that ionizes the surface of the disk shown in gray. The diffuse radiation from the inner disk ionizes the disk outside the critical radius r_g.

4.1.1 Angular Momentum Transport

One of the most active research fields on accretion disk theory is the study of mechanisms to explain the transport of angular momentum and accretion onto the central object. Protoplanetary disks rotate differentially and due to viscous stresses angular momentum is transported outwards. However, viscosity due to molecular transport is generally negligible and the concept of enhanced α-turbulence in accretion disks was introduced by Shakura & Syunyaev (1973) to account for the observed enhanced viscosity. The anomalous viscosity can be given by

$$\nu = \alpha c_s H, \tag{4.2}$$

where c_s denotes the sound speed, H is the scale height of the disk and α is a dimensionless parameter.

The magnetorotational instability has been proposed to explain the enhanced viscosity in hot and sufficiently ionized accretion disks threaded by a weak magnetic field (Balbus & Hawley 1991; Balbus et al. 1996; Balbus & Hawley 1998). However, in the context of cold protoplanetary disks, the ionization by cosmic rays and stellar radiation is limited to the surface layers of the disk while the so called “dead zone” in the vicinity of the central plane is expected to have low ionization (Gammie 1996). Fig. 4.2 shows a protoplanetary disk with a neutral dead zone and actively accreting layers. In cataclysmic variables and outer regions of active galactic nuclei the coupling

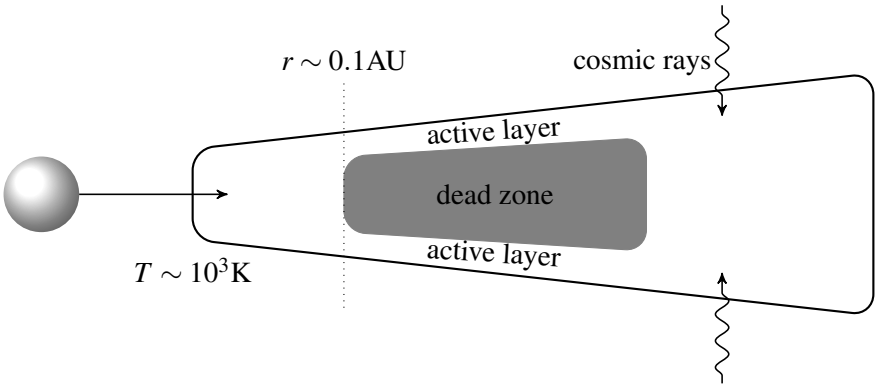

Figure 4.2: Sketch of the layered accretion model (Gammie 1996) in a protoplanetary disk with a neutral dead zone and active accreting layers above the midplane. The gas is ionized by stellar radiation and cosmic rays.

between the magnetic field and the gas is also weak and the MHD effects may be negligible.

Several mechanisms have been advanced that can sustain purely hydrodynamic turbulence and generate an anomalous α-viscosity. One possible source of hydrodynamic turbulence is the so-called baroclinic instability (Klahr & Bodenheimer 2003).

4.1.2 Vortex formation

Vortices in protoplanetary disks can capture solid particles and form planetary cores within shorter timescales than those involved in the standard core-accretion model. Dust particles trapped in vortices have an increased efficiency for binary agglomeration or can lead to a local gravitational instability (Barge & Sommeria 1995). In addition, vortices are able to transport angular momentum outwards in cold and unmagnetized protoplanetary disks.

The presence of vortices in protoplanetary disks can change the planet orbital migration rate when the gravitational torque from the vortex on the planet is sufficiently strong. Furthermore, giant planet migration is dependent on the disk viscosity, which can be modified by the presence of vortices. Numerical simulations of disk-planet interaction usually employ an enhanced viscosity and do not consider angular momentum transport due to vortices.

5. Planet-disk Interaction

Migration of protoplanets in disks has been predicted in the 1980's prior to the discovery of extrasolar planets. After the detection of giant planets in close orbits, planetary migration was invoked to explain their occurrence since it seems unlikely that gas giants could form close to their parent stars. Instead, planets are thought to have formed at much greater distances and then migrated to their present short-period orbits. Certain substances such as water and methane can only be found as solid ices at large distances from the star where it is cold enough and there they can agglomerate with the dust grains. Moreover, it is difficult for a planetary core in a tight orbit to accumulate enough gas to provide the atmosphere of a Jupiter-like planet. The gas in the disk is hotter close to the star and therefore less likely to be captured by a protoplanet. Also, a planet in a close orbit travels through a smaller volume of space than one in a large orbit does and has access to a smaller gas reservoir.

Different theories have been proposed which allow planets to migrate inward from several AU to where they are detected today. Most migration mechanisms consider the gravitational interactions between the protoplanet and the planetesimals, planets and the gaseous disk or the interactions between planets in a formed planetary system. We will only consider the planet-disk interaction in this section. Orbital migration due to gravitational planet-disk interaction was first proposed by Goldreich & Tremaine (1979, 1980). The subject of disk interactions was studied in the context of planetary rings and satellites before the discovery of extrasolar planets. The interaction between the disk and its protoplanets play an important role in the structure and evolution of the system. The gravitational tides raised in the disk by the planet produce changes in the density distribution in the disk which in turn exert a force on the planet. In particular, if the planet is massive enough, a gap opens up in the disk. A planet exchanges angular momentum with the disk at the so-called Lindblad and corotation resonances. Numerical simulations show that planets are able to move long distances from their birthplaces via spiraling orbits caused by the tidal interaction with the disk and the sign of the total torque determines the direction in which the planet migrates.

The gas flow in a disk with an embedded giant planet on a circular orbit is presented in Fig. 5.1. It has been suggested that planets can be detected from signatures in their spectra or particle outflows in debris disks (Moro-Martín et al. 2005; Moro-Martín & Malhotra 2005). Recent protoplanetary

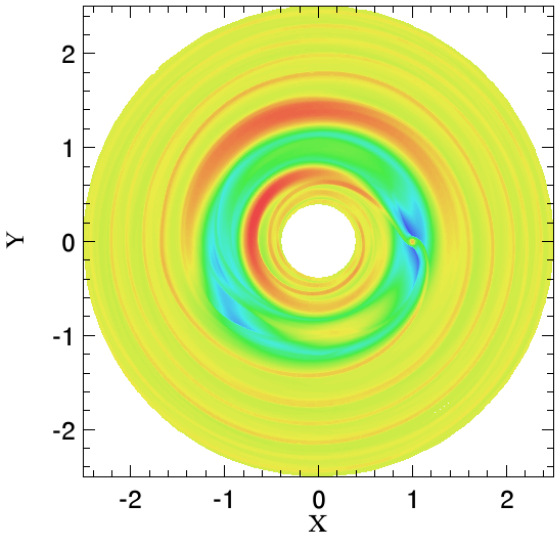

Figure 5.1: A Jupiter-mass planet at $(x,y) = (1,0)$ excites density waves and clears a gap in a 2-dimensional numerical model of a protoplanetary disk. Computer simulations have confirmed that tidal interactions between the planet and the disk can cause the planet to migrate.

disk observations suggest that the structure of disks is changed by embedded planets and the influence of the disk drives the planet orbital migration.

5.1 Resonances

The planetary potential can be expanded as a Fourier series in polar coordinates with the star located in the origin

$$\Phi(r,\phi,t) = \sum_m \psi_m(r)\cos(m\phi - m\Omega_p t), \tag{5.1}$$

where ψ is a radius-dependent amplitude and Ω_p is the angular velocity of the planet, which we have assumed to be on a circular orbit for simplicity. Each potential component is constant in a frame rotating with the angular velocity of the planet, so the induced perturbations of the disk's energy and angular momentum preserve the Jacobi constant:

$$\frac{dE}{dt} = \Omega_p \frac{dL}{dt} = \Omega_p T, \tag{5.2}$$

where E denotes energy per unit mass, L denotes specific angular momentum and T is the tidal torque exerted by the disk.

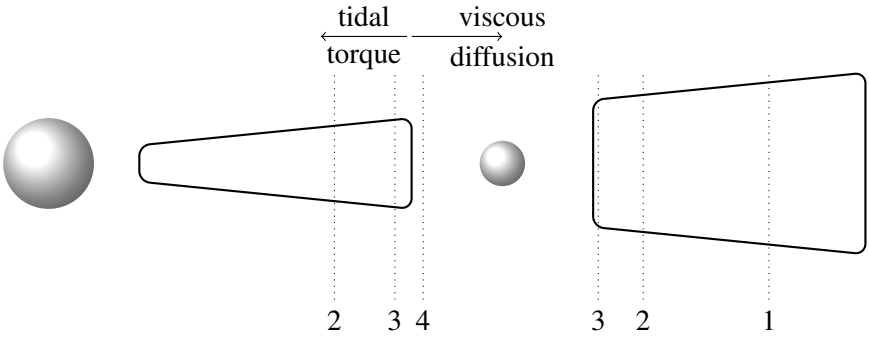

Figure 5.2: Illustration of the viscous condition for gap formation. A planet opens a gap when the tidal torques time scale for opening a gap becomes shorter than the viscous diffusion time scale. Dotted lines give the locations of the low order Lindblad resonances. The waves excited at the Lindblad resonances carry angular momentum through the disk.

The response of the disk to the planet occurs at various resonances, where tidal waves are excited. Two kinds of resonances can be distinguished: corotation resonances and Lindblad resonances. Both occur where the angular velocity in the disk, Ω_d, is related in a simple way to the angular velocity of the planet. Corotation resonances occur when $\Omega_d = \Omega_p$, while Lindblad resonances occur when

$$(\Omega_d - \Omega_p)m = \pm\kappa_d, \tag{5.3}$$

where κ_d is the epicyclic frequency of the disk, which is equal to Ω_d for a Keplerian disk. Inner and outer resonances are given by the plus and minus sign in the formula respectively. The planet-disk tidal interaction leads to the excitation of density waves and formation of spiral shocks at the Lindblad resonances. The redistribution of the angular momentum deposited by the planet at resonances leads to the planet gaining angular momentum from interacting with the inner disk, and losing angular momentum from interacting with the outer disk. The contribution from the outer disk usually dominates and the planet migrates inwards.

The planet does not excite any density waves at the corotation resonance and it is often assumed that this resonance saturates quickly. However, giant planets can undergo rapid migration directed both inwards and outwards due to the coorbital torque (Masset & Papaloizou 2003). Pepliński et al. (2008) showed that for massive disks the corotation resonance becomes the main driving force for planetary migration.

5.2 Type I Migration

Type I migration is a relatively quick ($10^5 - 10^6$ yr) migration of a small planet ($\sim M_\oplus$) still embedded in a protoplanetary disk. The angular momentum transport in the disk due to the tidal interaction with the planet is negligible, therefore the surface density is largely unperturbed. Type I migration has been defined as a regime of weak disk-planet interaction (Ward 1997).

The direction of the migration depends on the accurate calculation of competing torques on the planets. Korycansky & Pollack (1993) showed that for a significant fraction of phase space, this migration is inward. Nevertheless, for high disk opacities (Paardekooper & Mellema 2006) and an eccentric disk (Papaloizou 2002), migration can be directed outward.

A great effort has been committed to try to explain why the Earth-mass cores do not collide with the central star before the dissipation of the disk due to rapid inward migration. Nelson & Papaloizou (2004) investigated the interaction between a turbulent disc and a low-mass planetary companion and found that the density fluctuations generated by MHD turbulence can significantly modify planetary migration leading to a process known as stochastic migration.

Rice & Armitage (2003) have studied the effect of turbulent fluctuations on the formation of giant planets from Earth-mass planetary cores. Giant planet formation can be significantly more efficient if the planetary cores carry out a random walk with an amplitude of a few tenths of an AU.

5.3 Type II Migration

Massive planets are able to remove gas from the co-orbital region and open a gap in the disk due to angular momentum deposited at resonances. The surface density in the gap is much smaller than for an unperturbed disk. In order to be able to open a gap, the Hill sphere of the planet needs to be of the order of the disk thickness, a condition which is satisfied for planets more massive than 10^{-4} the mass of their star.

The Hill sphere is defined as the region where the gravitational influence of the planet dominates. The radius of the Hill sphere (or Roche radius) is given by the formula

$$R_H = a \left(\frac{M_\mathrm{p}}{3M_*} \right)^{1/3}, \tag{5.4}$$

where a is the planet's semimajor axis, M_p is the planet's mass and M_* represents the stellar mass.

The shape of the gap is determined by the balance between tidal forces that tend to open a gap, and viscous and pressure forces that try to close it (see e.g. Goldreich & Tremaine 1980). The viscous condition for gap opening is illustrated in Fig. 5.2. For typical disk parameters, the viscous condition for

gap opening is satisfied for a planet with mass ratio $\sim 10^{-4}$. Both the scale height and viscous condition give similar answers for the minimum mass for type II migration.

Once a planet opens a gap in the disk, its orbital migration happens on the viscous time scale. The radial velocity of the gas is given by

$$v_{\rm r} = -\frac{3}{2}\frac{\nu}{r}, \tag{5.5}$$

where ν is the kinematical viscosity and r is the radial distance.

6. Numerical Simulations of Disks with Planets

The dynamics of astrophysical systems such as accretion disks or supernova explosions involve nonlinear processes that cannot be calculated analytically so numerical simulations are important tools to study fluid flows in many astrophysical objects. The extreme conditions found in astrophysics such as highly compressible flows and strong shocks have been major drivers for the development of new numerical algorithms for fluid dynamics. With current computer capabilities, scientists are able to study astrophysical phenomena using numerical simulations in a similar way to laboratory experiments. In this chapter, we will discuss some of the numerical methods frequently used to simulate astrophysical fluids, with particular attention to simulations of disk-planet interaction.

The equations of hydrodynamics are presented in Section 6.1. In Section 6.2 we describe grid-based Eulerian schemes such as upwind and shock-capturing codes. We consider particle codes in Section 6.3.

6.1 Navier-Stokes equations

The fundamental differential equations that govern fluid dynamics are the Navier-Stokes equations (see e.g. Landau & Lifshitz 1959)

$$\frac{\partial \rho}{\partial t} + \nabla \cdot (\rho \mathbf{v}) = 0 \tag{6.1}$$

$$\frac{\partial \mathbf{v}}{\partial t} + (\mathbf{v} \cdot \nabla)\mathbf{v} = -\frac{1}{\rho}\nabla P - \nabla \Phi + \nabla \cdot \mathsf{T} \tag{6.2}$$

$$\frac{\partial E}{\partial t} + (\mathbf{v} \cdot \nabla)E = -\frac{P}{\rho}\nabla \cdot \mathbf{v} + \nabla(K \nabla T) \tag{6.3}$$

where ρ is the density, $\mathbf{v}$ the velocity of the fluid, P the pressure, Φ the gravitational potential, T is the full viscous stress tensor (e.g. Mihalas & Weibel Mihalas 1984), E the total energy, T the temperature and K the thermal conductivity coefficient. The first equation describes the conservation of mass, the second is conservation of momentum and lastly the energy equation. In the alternative integral representation of the Navier-Stokes equations, the rate of change of the conserved variables is given by the flux across the surface surrounding the control volume. The differential form of the equations is not

defined at shocks and can only be used for smooth flows, while the integral form can also account for discontinuities.

The dissipative terms in the Navier-Stokes equations depend on the second derivative of the velocity and temperature and make the differential equations parabolic. When viscosity and heat conduction are neglected in Eq. 6.3 we obtain the Euler equations. Radiation source terms usually need to be added to the equations in astrophysical applications.

An equation of state closes the system of equations. In astrophysical disks the mean free path of fluid particles is much smaller than the dimensions of the system. Therefore, it is possible to use an ideal equation of state to describe the fluid with additional terms for cooling and heating

$$P = (\gamma - 1)\varepsilon, \tag{6.4}$$

where ε is the thermal energy and γ is the ratio of specific heats given by

$$\gamma = \frac{\rho}{P}\frac{\partial P}{\partial \rho} = \frac{\rho}{P}c_{\rm s}^2, \tag{6.5}$$

where $c_{\rm s}$ is the sound speed. For a monoatomic gas with 3 internal degrees of freedom, $\gamma = 5/3$, which is frequently used in astrophysical simulations. The total energy of the fluid is defined as the sum of the kinetic energy per unit mass and thermal energy:

$$E = \frac{1}{2}v^2 + \varepsilon. \tag{6.6}$$

Radiative source terms in the energy equations account for emitted or absorbed radiation that usually require an integral over the entire domain. In the optically thin limit, radiation is assumed to escape without being absorbed within the computational domain. A locally isothermal equation of state can be used for optically thin cooling. This approximation is frequently used to study protoplanetary disks and molecular clouds, where heat generated by shocks is quickly radiated away.

One of the most demanding problems in numerical hydrodynamics is to resolve shock waves which often occur in astrophysical problems. The Navier-Stokes equations are not defined at discontinuities where derivatives are infinite and are only valid for smooth flows. Shock-capturing methods have been developed in the Eulerian and Lagrangian formulation to achieve high resolution shock capturing and to avoid unphysical instabilities near discontinuities (see Section 6.2 below).

Hydrodynamic codes are tested against problems such as the shock tube and Sedov blast wave, which have known analytical solutions. However, the problem of disk-planet interactions have different and more complex conditions than those simple tests. Paper I describes a comparison of 17 numerical schemes on the problem of a planet in a circumstellar disk.

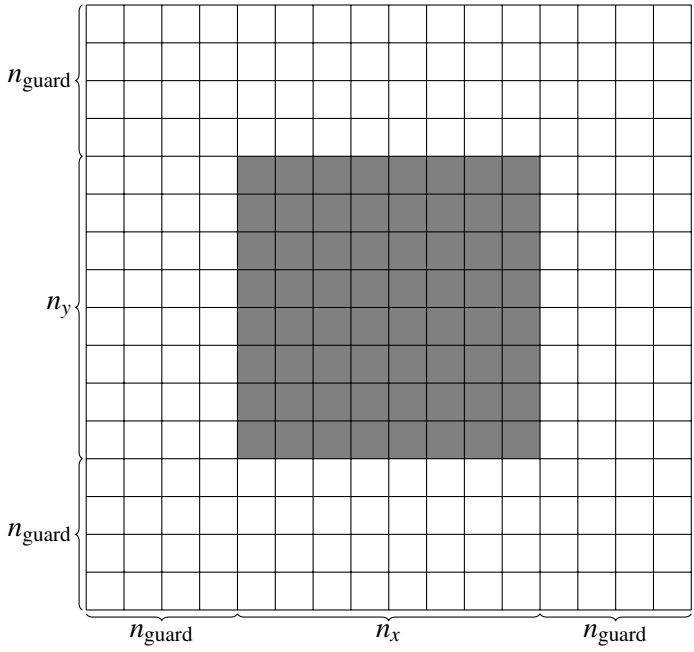

Figure 6.1: Structure of a 2-dimensional block in FLASH. The inner cells are marked in gray.

6.2 Grid Based Codes

The standard approach in Eulerian numerical hydrodynamics is to discretize the computational domain into finite cells at which the cell-averaged flow variables are stored. The equations are evolved in time with finite time steps satisfying the Courant-Friedrichs-Lewy (CFL) condition. In conservative schemes, the flux of mass, momentum and energy through a cell boundary is added to the adjacent cell. Fig. 6.1 shows the inner and guard cells in a block-structured grid-based code. For a recent review of Eulerian methods in computational fluid dynamics see Trac & Pen (2003).

Eulerian methods have a large dynamic range in mass but not in length and are able to resolve Kevin-Helmholtz and Rayleigh-Taylor instabilities (Agertz et al. 2007).

There is a wide range of spatial scales in typical astrophysical problems and non-uniform or adaptive grids are often needed. Adaptive grids can locally improve the resolution by several orders of magnitude, and are able to resolve well shocks and discontinuities. This method is known as adaptive mesh refinement (AMR). AMR codes can change the regions of refinement with time based on the behavior of the solution. Fluxes of conserved quantities should be conserved at the interface between coarse and fine grids. In Fig. 6.2, flux conservation across jumps in refinement is shown.

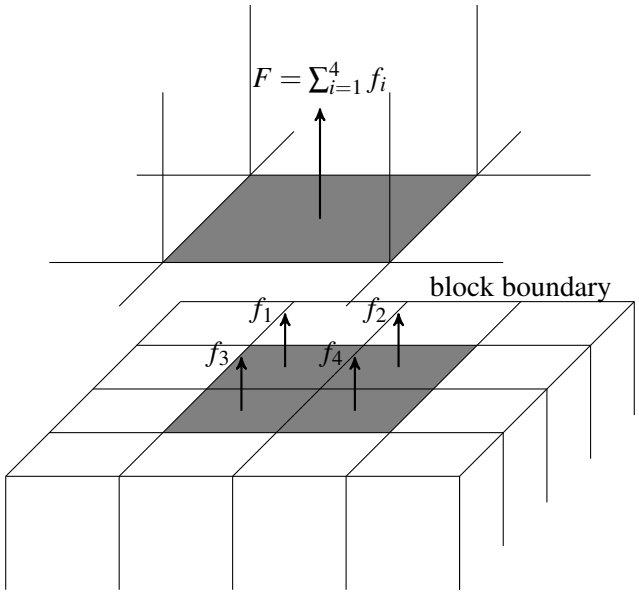

Figure 6.2: Flux consevation at jumps in refinement in AMR codes.

Finite Difference Methods

The finite difference method discretize the derivatives in the fluid equations to obtain a system of algebraic equations that can be solved numerically. We will consider the 1-dimensional Euler equation in differential form

$$\frac{\partial u}{\partial t} + \frac{\partial F(u)}{\partial x} = 0, \tag{6.7}$$

where u represents a conserved physical quantity and $F(u) = vu$ is the flux term with a constant v advection velocity. The analytical solution to this equation is given by

$$u(x,t) = u(x - vt, 0) \tag{6.8}$$

which represents the advection of the variable u with constant velocity v.

The conserved variables and fluxes are usually defined at the cell centers ($u_{\rm n}$ and $F_{\rm n}$). We will use a notation where subscript indices refer to the spatial dimension and superscript indices refer to time step. The solution of Eq. 6.7 at time $t + \Delta t$ can be obtained as

$$u_{\rm n}^{t+\Delta t} = u_{\rm n}^{t} - \left(\frac{F_{\rm n+1/2}^{t} - F_{\rm n-1/2}^{t}}{\Delta x} \right) \Delta t \ . \tag{6.9}$$

Finite difference methods calculate the fluxes at the cell boundaries $F_{\rm n+1/2}$ from the cell-averaged values.

In second-order centered method the fluxes at cell boundaries are estimated by

$$F_{\rm n+1/2}^{t} = \frac{F_{\rm n+1}^{t} + F_{\rm n}^{t}}{2} \ . \tag{6.10}$$

Then, the solution at time $t+\Delta t$ becomes

$$u_{\rm n}^{t+\Delta t} = u_{\rm n}^{t} - \left(\frac{F_{\rm n+1}^{t} - F_{\rm n-1}^{t}}{2\Delta x}\right)\Delta t \ , \tag{6.11}$$

or using the leapfrog method

$$u_{\rm n}^{t+\Delta t} = u_{\rm n}^{t-\Delta t} - \left(\frac{F_{\rm n+1}^{t} - F_{\rm n-1}^{t}}{\Delta x}\right)\Delta t \ . \tag{6.12}$$

However, this algorithms are numerically unstable, which can be shown using the von Neumann linear stability analysis.

Lax-Wendroff Method

The Lax-Wendroff approach is second-order accurate in both time and space. This method is based on the Taylor series expansion of $u(x,t+\Delta t)$

$$u(x,t+\Delta t) = u(x,t) + \Delta t\frac{\partial u(x,t)}{\partial t} + \frac{1}{2}\Delta t^2\frac{\partial^2 u(x,t)}{\partial t^2} + \mathscr{O}(\Delta t^3) \ . \tag{6.13}$$

If we replace time derivatives using Eq. 6.7, we obtain

$$u(x,t+\Delta t) = u(x,t) + \Delta t\frac{\partial F}{\partial x} + \frac{1}{2}\Delta t^2 v^2\frac{\partial^2 u(x,t)}{\partial x^2} + \mathscr{O}(\Delta t^3) \ . \tag{6.14}$$

Using central differences $u_n^{t+\Delta t}$ can be estimated by

$$u_{\rm n}^{t+\Delta t} = u_{\rm n}^{t} - \frac{\Delta t}{2\Delta x}(F_{\rm n+1}^{t} - F_{\rm n-1}^{t}) + \frac{\Delta t^2}{2\Delta x^2}v(F_{\rm n+1}^{t} - 2F_{\rm n}^{t} + F_{\rm n-1}^{t}) \ . \tag{6.15}$$

This is equivalent to using Eq. 6.9 where the fluxes at cell boundaries are given by

$$F_{\rm n+1/2}^{t} = \frac{1}{2}\left(F_{\rm n+1}^{t} + F_{\rm n}^{t}\right) - \frac{\Delta t}{2\Delta x}v\left(F_{\rm n+1}^{t} - F_{\rm n}^{t}\right) \ . \tag{6.16}$$

The stability of the Lax-Wendroff method can be shown using the Von Neumann stability analysis. Considering a Fourier series expansion for $u(x,t)$ of the form

$$u_{\rm n}^{t} = \frac{1}{N}\sum_{k=-N/2}^{N/2} c_k^t \exp\left(\frac{2\pi i k n}{N}\right) \ , \tag{6.17}$$

where N is the number of cells in our domain and c_k^t are the Fourier series coefficients that can be expressed as a plane wave

$$c_k^t = \exp\left(\frac{-2\pi i\omega t}{N}\right)c_k^{\circ} \ . \tag{6.18}$$

The stability condition $\mathrm{Im}(\omega) \leq 0$ is satisfied if

$$\frac{v\Delta t}{\Delta x} \leq 1 \ . \tag{6.19}$$

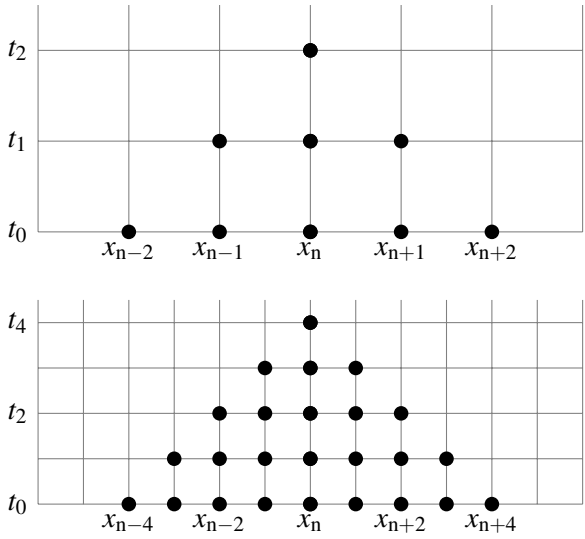

Figure 6.3: Domain of dependence using a Lax-Wendroff method on a 1-dimensional coarse and refined grid.

This is known as the CFL condition and is a necessary condition for convergence.

Lax-Wendroff schemes will be convergent when the numerical domain of dependence contains the true domain of dependece of a time-dependent differential equation. The domain of dependence shown in Fig. 6.3 is given by a range such that the initial values determine the solution over the full range. In the case of Eq. 6.7 the solution $u(x,t)$ depends on the value at $u(x-vt,0)$, therefore the domain of dependence of the point (x,t) is $x-vt$. For the Lax-Wendroff method the flux $F^t_{\rm n}$ depends on the values at $F^t_{\rm n-2}-2\Delta t,\ldots,F^t_{\rm n+2}-2\Delta t$ (see Figure 6.3).

A disadvantage of the Lax-Wendroff method is that it is extremely dispersive and can introduce spurious oscillations. To achieve high resolution and prevent artificial oscillations it is necessary to use nonlinear schemes.

Upwind Methods

These codes consider the physical conditions of the flow to estimate the fluxes at the cell boundaries depending on the sign of the velocity. The fulx at the cell boundaries is given by

$$F^t_{\rm n+1/2} = \begin{cases} F^t_{\rm n} & \text{if } v > 0 \\ F^t_{\rm n+1} & \text{if } v < 0\,. \end{cases} \tag{6.20}$$

The derivatives can be discretized in several ways, for example first-order upwind methods use

$$u_{\rm n}^{t+\Delta t} = u_{\rm n}^{t} - \left(\frac{F_{\rm n}^{t} - F_{\rm n-1}^{t}}{\Delta x} \right) \Delta t \tag{6.21}$$

for a positive velocity v where the fluid flows from left to right, and

$$u_{\rm n}^{t+\Delta t} = u_{\rm n}^{t} - \left(\frac{F_{\rm n+1}^{t} - F_{\rm n}^{t}}{\Delta x} \right) \Delta t \tag{6.22}$$

for negative velocity.

The CFL condition for first-order upwind codes can be calculated from the von Neumann stability analysis and is the same as for Lax-Wendroff schemes. First-order upwind methods are diffusive but they have the property of monotonicity preservation and do not produce artificial oscillations.

Shock-Capturing Methods

High-resolution shock-capturing methods for grid-based astrophysical flows were developed originally by Godunov (1959). These schemes make use of the fact that there is an analytic solution to the 1-dimensional shock tube problem of gas dynamics. The so-called Riemann problem can be expressed as an initial discontinuity in density and pressure with $\mathbf{v} = 0$

$$u(x) = \begin{cases} u_l & \text{if } x < 0 \\ u_r & \text{if } x > 0. \end{cases} \tag{6.23}$$

A shock wave propagates towards the region with lower pressure and is followed by a contact discontinuity across which the density is discontinuous but pressure and velocity are constant. Godunov's original scheme treated each cell as piecewise-constant and solved the Riemann problem between neighboring grid cells. Piecewise parabolic methods (PPM) are common implementation of the Godunov method using parabolic interpolation Woodward & Colella (1984); Colella & Woodward (1984). Implementations of PPM can be in Eulerian or Lagrangian form. Since solving the full Riemann problem is computationally expensive, many codes use an approximate solver.

6.3 Particle Based Codes

Lagrangian codes such as Smoothed Particle Hydrodynamics (SPH) methods decompose the flow into small fluid packets with fixed mass, instead of solving the fluid equations on a grid. The evolution of fluid particles is calculated using a Monte Carlo approximation to solve the fluid equations (Lucy 1977; Gingold & Monaghan 1977). Fluid variables in SPH methods are spread over a small

volume of space contained within a smoothing length. A typical smoothing function is the spline kernel:

$$W(r;h) = \frac{7}{10\pi h^2} \begin{cases} 1-(3v^2/2)+(3v^3/4) & \text{if } 0 \le v \le 1 \\ (2-v)^3/4 & \text{if } 1 \le v \le 2 \\ 0 & \text{elsewhere} \end{cases} \tag{6.24}$$

where $v = r/h$, with r the distance from the cell centre to the given particle and h the smoothing length of the particle. The density at a given position is calculated by interpolation with the spline kernel

$$\langle \rho(\mathbf{r}_\mathrm{i}) \rangle = \sum_{j=1}^{N} m_\mathrm{j} W(|\mathbf{r}_\mathrm{i} - \mathbf{r}_\mathrm{j}|, h_\mathrm{j}) \tag{6.25}$$

where m_j is the mass of the particle, $W(r,h_\mathrm{j})$ is the spline kernel and $|\mathbf{r}_\mathrm{i} - \mathbf{r}_\mathrm{j}|$ is the distance from the cell centre to the given particle. The smoothing length h_j has different values for each particle. A detailed description of SPH schemes is given in Benz (1990); Monaghan (1992).

The smoothing function (or kernel), $W(r,h)$, is not constant, but increases towards the particle's position (assumed to be $r = 0$). In the limit $h \to 0$, W becomes a δ-function, and perfect fluid behaviour is obtained (with an infinite number of particles). A Gaussian would be a possible choice for W, but compact kernels (where $W = 0$ for r greater than some r_max) are preferred for computational simplicity. Particles within the range of the compact kernel are called the neighbours. The smoothing length is also used to limit the timestep in a way similar to the CFL condition mentioned above.

Lagrangian schemes have a large dynamic range in length but not in mass, as opposed to Eulerian methods. The major advantage of SPH is that its particle nature makes it fully Lagrangian: there are no advective terms in the equations of motion. Since high densities imply that more particles are present, SPH naturally concentrates resolution in high density regions. Therefore, this method is well suited for core collapse simulations (see e.g. Delgado-Donate et al. 2003).

A disadvantage of SPH methods is that shocks are not captured and require the addition of artificial viscosity to prevent oscillations and inter-particle penetration. Artificial viscosity broaden shocks and therefore SPH codes tend to be more dissipative than grid-based codes. Lagrangian codes have high resolution in high density regions but poor resolution in low density regions where there are fewer particles, which can also be a problem in certain astrophysical problems such as protoplanetary disks. For example, the gap opened by a giant planet in a disk is not well resolved by SPH codes.

7. Wind Dynamics in Symbiotic Binaries

In this chapter we describe the Bondi-Hoyle-Lyttleton scenario and discuss wind dynamics in symbiotic binaries.

7.1 Bondi-Hoyle-Lyttleton accretion

Wind accretion by a compact object occurs in many astrophysical systems such as symbiotic binaries and massive X-ray binaries and can change the surface composition of the accreting companion and orbital parameters of the system. Hoyle & Lyttleton (1939) were the first to consider this problem for high velocity winds where the pressure can be neglected (see Edgar 2004, for a recent review of Bondi-Hoyle-Lyttleton accretion). The gas is gravitationally deflected on both sides and collide behind the gravitating object which accretes some of the material.

For a streamline with impact parameter ζ, a ballistic orbit where pressure is neglected will be described by

$$\ddot{r} - r\dot{\varphi}^2 = -\frac{GM}{r^2}, \tag{7.1}$$

$$r^2\dot{\varphi} = \zeta v_\infty. \tag{7.2}$$

A sketch of the geometry is shown in Fig. 7.1.

Assuming that the transverse velocity at the accretion wake cancels and that material bound to the star will be accreted, the accretion rate for a wind with uniform density ρ_∞ and velocity v_∞ is given by

$$\dot{M}_{\rm BH} = \pi R_{\rm a}^2 \rho_\infty v_\infty, \tag{7.3}$$

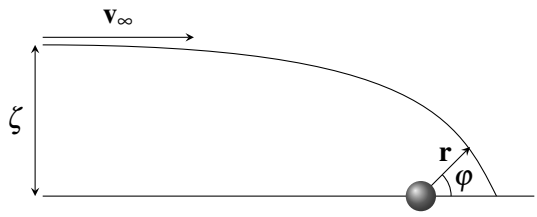

Figure 7.1: Diagram of the Bondi-Hoyle accretion picture.

where R_a is the Bondi-Hoyle accretion radius given by

$$R_a = \frac{2GM}{v_\infty^2}. \tag{7.4}$$

where G is the gravitational constant and M is the mass of the accretor. The wind material will be accreted for impact parameters $\zeta < R_a$.

If the gas pressure is included but the motion of the star with respect to the ambient medium is neglected, the mass accretion rate becomes (Bondi 1952; Theuns & David 1992)

$$\dot{M}_{BH} = \alpha \pi R_a^2 \rho_\infty c_s. \tag{7.5}$$

where α is a constant of order unity and c_s is the sound speed. The definition of the accretion radius is in this case

$$R_a = \frac{2GM}{c_s^2}. \tag{7.6}$$

When the pressure and motion of the gas are considered, the accretion rate is an interpolation of the previous expressions

$$\dot{M}_{BH} = \alpha \pi R_a^2 \rho_\infty v_\infty \left(\frac{\mathscr{M}^2}{1+\mathscr{M}^2} \right)^{3/2}, \tag{7.7}$$

where the accretion radius is defined as

$$R_a = \frac{2GM}{v_\infty^2 + c_s^2}, \tag{7.8}$$

and $\mathscr{M}$ denotes the Mach number

$$\mathscr{M} = \frac{v_\infty}{c_s}. \tag{7.9}$$

However, the Hoyle-Lyttleton theory cannot be directly applied to the wind accretion scenario in the case of slow winds where the accretion radius is comparable to the stellar separation. In this case, the fraction of the AGB wind accreted by the secondary can be several times higher than the Bondi-Hoyle rate in numerical simulations due to gravitational wind focusing.

7.2 Accretion in Symbiotic Binaries

Observations of symbiotic systems show complex and time-dependent structures with variability on time scales of the order of seconds to thousands of years (Walder & Folini 2000). A typical symbiotic consists of a mass-losing Asymptotic Giant Branch (AGB) star or red giant star and a hot accreting companion, often a white dwarf. Symbiotic binaries are important astrophysical laboratories to study wind accretion because of the possibility to observe

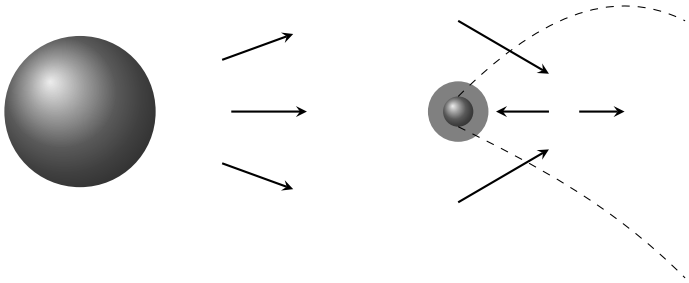

Figure 7.2: Diagram of the orbital plane of a wind accreting binary system. Gravitationally deflected material that has a velocity smaller than the escape velocity is accreted.

the individual components and the accretion processes at many wavelengths (Karovska et al. 1997, 2005; Matthews & Karovska 2006). Some of these systems have large outbursts which are related with the wind accretion dynamics.

An accretion disk around Mira B has been recently discovered via infrared data (Ireland et al. 2007). The disk is formed from material captured by Mira A's massive wind, with an accretion efficiency of about one percent. Planet formation is unlikely in an active accreting disk, although Ireland et al. (2007) suggest planets may form once Mira A completes its red giant phase and becomes a white dwarf.

7.3 Colliding winds

Different types of binary systems such as symbiotic binaries, systems containing a massive OB and Wolf-Rayet star and pulsar binaries may have colliding winds (Prilutskii & Usov 1976; Cherepashchuk 1976). Spatially resolved observations of wind-wind collisions have revealed spiral structures that are believed to match the collision region (Dougherty et al. 2005). Shocked and heated gas should produce a large X-ray luminosity that has been observed.

Multidimensional hydrodynamical simulations of colliding winds are very demanding computationally. Numerical models have confirmed that shocks are spirally shaped and limit high density regions and voids in the vicinity of the stars (Walder & Folini 2000).

8. Young Binary Systems

The formation of a binary system surrounded by a circumbinary disk is the most common result of stellar formation in molecular cores. Therefore, the study of accretion onto binary systems is one of the most important problems in star formation. High-resolution infrared observations of low-mass star forming regions have shown that multiple stars are common (Ghez et al. 1993). Recently, surveys of T Tauri stars have have allowd to estimate the frequency of multiple systems. (see Duchêne et al. 2007, and references therein). The binary frequency has been found to be higher in star-forming regions than in main-sequence stars.

Close binary stars form by fragmentation of dense cores and they accrete mass from the envelope via a circumbinary disk. Classical T Tauri stars (CTTS) are young pre-main-sequence objects with pronounced emission line spectra and IR excess emission from circumstellar disks. A number of CTTS are confirmed close binaries, with orbital periods of days to weeks, and several of these show emission lines that vary in intensity and line shape with phase. There is observational evidence that close binaries have dinamically truncated circumstellar disks that are replenished from an envelope or circumbinary disk. In such systems the stars orbit in a gap inside the circumbinary disk.

When the binary has an eccentric orbit, there may periodic changes in the accretion rate (Artymowicz & Lubow 1996). Eccentric systems, like DQ Tau (Basri et al. 1997) and UZ Tau E (Martín et al. 2005), show enhanced emission line activity close to periastron passages. This indicates that the accretion in such systems is non-axisymmetric, and perturbed by the orbital interaction with the inner disk.

Numerical simulations have been used to study fragmentation of molecular cores and evolution of young binary systems. These numerical models can be compared with observed systems. It is of interest to understand how the components in binaries evolve due to mass accretion from the circumbinary disk, and how the orbital elements may change with time. Protobinary systems allow us to study disk evolution under well defined conditions, since the sizes of the central gaps in the circumbinary disk are determined by tidal truncation and the stellar components are supposedly coeval. Numerical simulations of binary systems with a circumbinary disk based on Smoothed Particle Hydrodynamics (SPH) (Artymowicz & Lubow 1994; Bate & Bonnell 1997) and grid-based methods (Günther & Kley 2002; Günther et al. 2004) show that an

inner hole forms inside of the 2:1 resonance. Bate & Bonnell (1997) found that, in binaries with a mass ratio q different from unity, the less massive protostar accretes more material and is therefore more luminous. However, that claim has been refuted using high-resolution 2-dimensional simulations (Ochi et al. 2005; Sotnikova & Grinin 2007) For recent reviews of disks in young binaries see Mathieu et al. (2000); Duchêne et al. (2007).

Artymowicz & Lubow (1996) showed that binaries with eccentric orbits can generate non-axisymmetric gas flows from the disk edge related with periodic line changes observed in such systems. It was later pointed out that such flows appear also in systems with circular orbits (Artymowicz 2005; see Gahm 2006, page 151). Mass transfer occurs also in these systems but the gas density inside the gap is lower than for systems with eccentric orbits. However, low-eccentricity binaries should not experience accretion bursts (Artymowicz & Lubow 1996).

V4046 Sgr is a close T Tauri binary with an orbital period of 2.4 days and an eccentricity close to zero. Recently, Stempels & Gahm (2004) have observed spectroscopic features that can be explained by the presence of material in corotation with the central binary. These observations provide additional evidence for accretion from the circumbinary disk. This object shows pronounced periodic changes in the emission line profiles, which were related to gas orbiting between the stars and the disk edge and in corotation with the central binary by Stempels & Gahm (2004). The observations provide evidence that gas is flowing across the gap in young, close binary systems with circular orbits.

In paper IV, we investigate in detail the evolution of protoplanetary disks surrounding close T Tauri binaries with circular orbits and slightly different masses. The main goal of this paper is to make a comparison between accretion flows in our hydrodynamic model and spectroscopic observations of the CTTS binary system V4046 Sgr.

9. Summary of the Papers

In this chapter we describe the main results in the publications and studies in-progress included in this thesis. Papers I and II study the interaction between a gaseous disk and an embedded protoplanet using numerical and analytical methods. Disk-planet interactions are likely to play a key role in the formation and evolution of extrasolar planetary systems. In Paper III, we investigate accretion flows in wind accreting binary systems using 2-dimensional hydrodynamical simulations. Paper IV studies accretion processes and line emission in young binary systems with a circumbinary disk.

9.1 Paper I

In Paper I we present a detailed numerical comparison on the problem of planet-disk interactions. The standard test problems for hydrodynamic codes deal with problems that usually have very different conditions than those of the problem of a protoplanetary disk with an embedded planet. A comprehensive test of different numerical codes on a well defined problem was proposed in the framework of the EU network "Planets" and interested researchers were invited to join this comparison. The test problem was run with 17 independent codes and the data was analyzed and interpreted at Stockholm. Similar projects in different fields have been completed recently, including the Santa Barbara cosmological hydrocode comparison program (Frenk et al. 1999) and the non-LTE radiative transfer code comparison (van Zadelhoff et al. 2002).

We performed nonlinear global hydrodynamical simulations of disks with a giant planet with mass in the range Neptune to Jupiter-size. Future hydrodynamic codes may be benchmarked against the results presented in de Val-Borro et al. (2006) [1] We study the gravitational interaction between a protoplanetary disk and an a planet kept on a fixed circular orbit during several hundred orbital periods. We run tests for inviscid and viscous disks with Navier-Stokes viscosity of $\nu = 10^{-5}$ (in units of $a^2\Omega_p$). We find good agreement between different codes. The averaged density profiles agree within 5%. The smoothed total torques acting on the planet agree within a factor of 2 and the disk masses agree within 10% after 200 orbits. SPH results have comparable shape of the gap and weaker planetary wakes than grid-based codes.

[1] The comparison results are presented at http://www.astro.su.se/groups/planets/comparison.

Torque contributions from different parts in the disk and mass losses at the domain boundaries are monitored with high temporal resolution.

9.2 Paper II

Paper II focuses on the dynamics of planet formation in protoplanetary disk with special emphasis to the role of hydrodynamical disk instabilities. We use two different modern multi-dimensional hydrodynamical codes frequently used in modeling of protoplanetary disks. The non-linear hydrodynamical simulations are compared with a semianalytical linear modal analysis. High-density vortices are generated close to the coorbital region in the inviscid runs in agreement with the linear analysis. As the vortices move along the gap they introduce strong perturbations on the torque exerted on the planet.

Modal analysis shows that unstable modes are generated with growth rates of order $0.3\Omega_K$ for low-order azimuthal numbers $m = 4, \ldots, 6$, where Ω_K is the local Keplerian frequency. The instability is a robust mechanism and can be sustained for log time scales. When there is a sufficiently strong Navier-Stokes viscosity of the order $\nu = 10^{-5}$ the growth of unstable modes is prevented. These studies are also relevant for our understanding of other astrophysical systems such as cataclysmic variables, accretion disks around stellar mass black holes and young binary stars surrounded by circumbinary disks.

9.3 Paper III

Paper II studies accretion processes in wind accreting binaries, including dynamical effects on winds due to gravitational focusing by a compact companion. We investigate the mass transfer and formation of bow shocks and accretion disks around the secondary in detached systems consisting of a mass-losing evolved star and a compact accreting companion. We developed 2-dimensional hydrodynamical models to study accretion flow between the components and formation of accretion disks as a function of mass loss rate, wind temperature and orbital parameters. The numerical code is based on FLASH and uses an adaptive mesh refinement method that provides higher resolution at the position of the secondary.

Our results show that the massive and slow wind from an evolved star is significantly focused towards the companion and Roche lobe overflow-like accretion for several wind and orbital parameters. There is enhanced accretion onto the compact object with respect to the Bondi-Hoyle estimate for a range of wind parameters and dust profiles. This effect has consequences on accretion disk formation and evolution of binary system and its individual components.

9.4 Paper IV

In Paper IV we study the evolution of close T Tauri binaries surrounded by a circumbinary disk. We use hydrodynamic 2-dimensional simulations to study the accretion flows from the circumbinary disk onto the stellar components. Although there is substantial accretion across the low-density gap onto the stars in a time-dependent manner, the inner cavity remains open after several orbital periods. We find that the circumstellar disk around the primary is significantly more massive than the disk around the secondary when the system has reached a quasistatic state in agreement with the simulations of Ochi et al. (2005).

We calculate line emission profiles from the circumstellar disks and accretion streams onto the components of the close T Tauri binary V4046 Sagittarii as a function of orbital phase. The shape of the line profiles is estimated decoupled from the hydrodynamical simulations assuming the intensity for each velocity bin is proportional to the surface density squared. We fit the theoretical profiles using four components from inside the circumbinary gap as observed in the hydrogen line profiles (Stempels & Gahm 2004). There is qualitative agreement between our calculated profiles and the observed line profiles of V4046 Sgr at some orbital phases.

Acknowledgements

I am grateful to my supervisor at Stockholm Observatory, Pawel Artymowicz, who first introduced me to the field of planet formation. His guidance and expertise helped me along the way and motivated this project. I would like to thank warmly all the members of the "Planetary Systems" group. Richard Edgar provided advice and support for the code comparison project and guided the project in the right direction. I am very thankful to Gennaro D'Angelo for his excellent guidance and helpful discussions. Adam Peplinski, Philippe Thebault, Eduardo Delgado-Donate, Artur Gawryszczak and Garrelt Mellema provided insightful comments on my work and support. I would like to acknowledge the contributions from all the co-authors in the code comparison project, your help and encouragement are greatly appreciated. I am very grateful to Gösta Gahm and Eric Stempels for their collaboration on modeling of circumbinary disks and help with the interpretation of the hydrodynamical simulations. I would like to thank my thesis advising committee at Stockholm Observatory, Claes-Ingvar Björnsson and Claes Fransson, for valuable suggestions and keeping my thesis projects on the right track. I am also grateful to the High-energy Astrophysics group at Stockholm Observatory for having me as a student. Sergio Gelato and the computer support group were always helpful to solve my computer problems. I have enjoyed very much the company of my fellow graduate students at Stockholm Observatory and received constructive support from them. Special thanks go to Lena Olofsson, Ulla Engberg, Sandra Åberg and Uno Wänn for always being very helpful.

I wish to express my gratitude to the Institute for Theory and Computation and the Solar, Stellar and Planetary Sciences Division at the Harvard-Smithsonian Center for Astrophysics for having me as SAO predoctoral fellow. I am specially indebted to my advisers at the CfA, Dimitar Sasselov, Margarita Karovska and Matthew Holman, for valuable mentoring and continuous support. Special thanks go to Joe Barranco, Mike Lecar, Morris Podolak and Robert Marcus for helpful comments and an interesting collaboration. I have enjoyed conversations with my roommates at the ITC Tommy Grav and Desika Narayanan. Nayla Rathle and Christine Crowley were of great help with administrative matters and all kinds of useful advice. Lucas Salazar provided helpful assistance and made my stay in Boston very enjoyable.

I am also very grateful to the EU Planets network coordinated by Andreas Burkert from Munich Observatory for providing funding for a workshop on

"Numerics of planet-disk interaction" held in Stockholm to discuss the results of the code comparison project.

During my undergraduate studies at University of Salamanca I was lucky to have very enthusiastic and dedicated teachers. In particular, I am very grateful to my advisor at Salamanca, Fernando Atrio-Barandela, for introducing me to astronomy research and his continuous support and encouragement.

Last but not least I would like to thank my family for their constant support over the years.

Publications not included in this thesis

V de Val-Borro, M. (2003) Turbulence and instabilities in protoplanetary disks, IAU Symposium 221 *Star Formation at High Angular Resolution*

VI Borgonovo, L., Ryde, F., de Val Borro, M. & Svensson, R. (2003) Determining Bolometric Corrections for BATSE Burst Observations, *Gamma-Ray Burst and Afterglow Astronomy 2001*, ed. G. R. Ricker & R. K. Vanderspek (New York: AIP)

VII de Val-Borro, M. & Artymowicz, P. (2004) Instabilities and Vorticity Generation in Protoplanetary Disks, ASP Conf. Series 321, *Extrasolar Planets: Today and Tomorrow*, eds. J. Beaulieu, A. Lecavelier Des Etangs & C. Terquem

VIII de Val-Borro, M., Edgar, R. G., Artymowicz, P., Ciecielag, P., Cresswell, P., D'Angelo, G., Delgado-Donate, E. J., Dirksen, G., Fromang, S., Gawryszczak, A., Klahr, H., Kley, W., Lyra, W., Masset, F., Mellema, G., Nelson, R. P., Paardekooper, S.-J., Peplinski, A., Pierens, A., Plewa, T., Rice, K., Schäfer, C., Speith, R. (2007) A numerical comparison of disk-planet interactions, *Bulletin of the American Astronomical Society*, DPS meeting 39, 42.05

Bibliography

Agertz, O. et al. 2007, MNRAS, 380, 963, arXiv:astro-ph/0610051

Alexander, R. D., Clarke, C. J., & Pringle, J. E. 2006, MNRAS, 369, 229, arXiv:astro-ph/0603254

André, P. 1994, in The Cold Universe, ed. T. Montmerle, C. J. Lada, I. F. Mirabel, & J. Tran Thanh van, 179–+

Armitage, P. J. 2007, ArXiv Astrophysics e-prints, astro-ph/0701485

Artymowicz, P. 2005, privative communication

Artymowicz, P., & Lubow, S. H. 1994, ApJ, 421, 651

——. 1996, ApJ, 467, L77

Bailes, M., Lyne, A. G., & Shemar, S. L. 1991, Nature, 352, 311

Balbus, S. A., & Hawley, J. F. 1991, ApJ, 376, 214

——. 1998, Reviews of Modern Physics, 70, 1

Balbus, S. A., Hawley, J. F., & Stone, J. M. 1996, ApJ, 467, 76

Baraffe, I., Selsis, F., Chabrier, G., Barman, T. S., Allard, F., Hauschildt, P. H., & Lammer, H. 2004, A&A, 419, L13, arXiv:astro-ph/0404101

Barge, P., & Sommeria, J. 1995, A&A, 295, L1, arXiv:astro-ph/9501050

Basri, G., Johns-Krull, C. M., & Mathieu, R. D. 1997, AJ, 114, 781

Bate, M. R., & Bonnell, I. A. 1997, MNRAS, 285, 33

Beaulieu, J.-P. et al. 2006, Nature, 439, 437, arXiv:astro-ph/0601563

Benz, W. 1990, in Numerical Modelling of Nonlinear Stellar Pulsations Problems and Prospects, ed. J. R. Buchler, 269

Beuzit, J.-L., Mouillet, D., Oppenheimer, B. R., & Monnier, J. D. 2007, in Protostars and Planets V, ed. B. Reipurth, D. Jewitt, & K. Keil, 717–732

Bondi, H. 1952, MNRAS, 112, 195

Boss, A. P. 2001, ApJ, 563, 367

Butler, R. P. et al. 2006, ApJ, 646, 505, arXiv:astro-ph/0607493

Cabrera, J., & Schneider, J. 2007, in Astronomical Society of the Pacific Conference Series, Vol. 366, Transiting Extrapolar Planets Workshop, ed. C. Afonso, D. Weldrake, & T. Henning, 242–+

Charbonneau, D., Brown, T. M., Noyes, R. W., & Gilliland, R. L. 2002, ApJ, 568, 377, arXiv:astro-ph/0111544

Cherepashchuk, A. M. 1976, Soviet Astronomy Letters, 2, 138

Chiang, E., Lithwick, Y., Murray-Clay, R., Buie, M., Grundy, W., & Holman, M. 2007, in Protostars and Planets V, ed. B. Reipurth, D. Jewitt, & K. Keil, 895–911

Colella, P., & Woodward, P. 1984, J. Comput. Phys., 54, 174

de Val-Borro, M. et al. 2006, MNRAS, 370, 529, arXiv:astro-ph/0605237

Delgado-Donate, E. J., Clarke, C. J., & Bate, M. R. 2003, MNRAS, 342, 926, arXiv:astro-ph/0304091

Dick, S. J. 1982, Plurality of worlds : the origins of the extraterrestrial life debate from Democritus to Kant (Cambridge [Cambridgeshire] ; New York : Cambridge University Press, 1982.)

Dominik, C., Blum, J., Cuzzi, J. N., & Wurm, G. 2007, in Protostars and Planets V, ed. B. Reipurth, D. Jewitt, & K. Keil, 783–800

Dougherty, S. M., Beasley, A. J., Claussen, M. J., Zauderer, B. A., & Bolingbroke, N. J. 2005, ApJ, 623, 447, arXiv:astro-ph/0501391

Drake, F. D. 1962, Intelligent life in space. (New York, Macmillan [1962])

Duchêne, G., Delgado-Donate, E., Haisch, Jr., K. E., Loinard, L., & Rodríguez, L. F. 2007, in Protostars and Planets V, ed. B. Reipurth, D. Jewitt, & K. Keil, 379–394

Edgar, R. 2004, New Astronomy Review, 48, 843, arXiv:astro-ph/0406166

Ford, E. B. 2004, PASP, 116, 1083, arXiv:astro-ph/0412341

Ford, E. B., & Gaudi, B. S. 2006, ApJ, 652, L137, arXiv:astro-ph/0609298

Ford, E. B., & Holman, M. J. 2007, ApJ, 664, L51, arXiv:0705.0356

Frenk, C. S. et al. 1999, ApJ, 525, 554, arXiv:astro-ph/9906160

Gahm, G. 2006, Ap&SS, 304, 149

Gammie, C. F. 1996, ApJ, 457, 355

Ghez, A. M., Neugebauer, G., & Matthews, K. 1993, AJ, 106, 2005

Gingold, R. A., & Monaghan, J. J. 1977, MNRAS, 181, 375

Godunov, S. K. 1959, Mat. Sb., 47, 271

Goldreich, P., & Tremaine, S. 1979, ApJ, 233, 857

——. 1980, ApJ, 241, 425

Goldreich, P., & Ward, W. R. 1973, ApJ, 183, 1051

Günther, R., & Kley, W. 2002, A&A, 387, 550, arXiv:astro-ph/0204175

Günther, R., Schäfer, C., & Kley, W. 2004, A&A, 423, 559, arXiv:astro-ph/0405053

Hartmann, L. 1998, Accretion Processes in Star Formation (Accretion processes in star formation / Lee Hartmann. Cambridge, UK ; New York : Cambridge University Press, 1998. (Cambridge astrophysics series ; 32) ISBN 0521435072.)

Hoyle, F., & Lyttleton, R. A. 1939, in Proceedings of the Cambridge Philosophical Society, Vol. 35, Proceedings of the Cambridge Philosophical Society, 405–+

Ireland, M. J. et al. 2007, ApJ, 662, 651, arXiv:astro-ph/0703244

Karovska, M., Hack, W., Raymond, J., & Guinan, E. 1997, ApJ, 482, L175

Karovska, M., Schlegel, E., Hack, W., Raymond, J. C., & Wood, B. E. 2005, ApJ, 623, L137, arXiv:astro-ph/0503050

Kenyon, S. J., & Hartmann, L. 1987, ApJ, 323, 714

Klahr, H. H., & Bodenheimer, P. 2003, ApJ, 582, 869, arXiv:astro-ph/0211629

Korycansky, D. G., & Pollack, J. B. 1993, Icarus, 102, 150

Landau, L. D., & Lifshitz, E. M. 1959, Fluid mechanics (Course of theoretical physics, Oxford: Pergamon Press, 1959)

Larson, R. B. 2003, Reports of Progress in Physics, 66, 1651, arXiv:astro-ph/0306595

Lissauer, J. J. 1993, ARA&A, 31, 129

Lucy, L. B. 1977, AJ, 82, 1013

Marcy, G., Butler, R. P., Fischer, D., Vogt, S., Wright, J. T., Tinney, C. G., & Jones, H. R. A. 2005, Progress of Theoretical Physics Supplement, 158, 24, arXiv:astro-ph/0505003

Marcy, G. W., & Butler, R. P. 1998, ARA&A, 36, 57

Martín, E. L., Magazzù, A., Delfosse, X., & Mathieu, R. D. 2005, A&A, 429, 939, arXiv:astro-ph/0409449

Masset, F. S., & Papaloizou, J. C. B. 2003, ApJ, 588, 494, arXiv:astro-ph/0301171

Mathieu, R. D., Ghez, A. M., Jensen, E. L. N., & Simon, M. 2000, Protostars and Planets IV, 703, arXiv:astro-ph/9909424

Matthews, L. D., & Karovska, M. 2006, ApJ, 637, L49, arXiv:astro-ph/0512205

Mayor, M., & Queloz, D. 1995, Nature, 378, 355

McKee, C. F., & Ostriker, E. C. 2007, ARA&A, 45, 565, arXiv:0707.3514

Mihalas, D., & Weibel Mihalas, B. 1984, Foundations of radiation hydrodynamics (New York: Oxford University Press, 1984)

Mizuno, H. 1980, Progress of Theoretical Physics, 64, 544

Monaghan, J. J. 1992, ARA&A, 30, 543

Moro-Martín, A., & Malhotra, R. 2005, ApJ, 633, 1150, arXiv:astro-ph/0506674

Moro-Martín, A., Wolf, S., & Malhotra, R. 2005, ApJ, 621, 1079, arXiv:astro-ph/0506669

Murray, C. D., & Dermott, S. F. 2000, Solar System Dynamics (Cambridge University Press)

Nelson, R. P., & Papaloizou, J. C. B. 2004, MNRAS, 350, 849, arXiv:astro-ph/0308360

Ochi, Y., Sugimoto, K., & Hanawa, T. 2005, ApJ, 623, 922

Paardekooper, S.-J., & Mellema, G. 2006, A&A, 459, L17, arXiv:astro-ph/0608658

Papaloizou, J. C. B. 2002, A&A, 388, 615, arXiv:astro-ph/0204197

Papaloizou, J. C. B., & Terquem, C. 2006, Reports of Progress in Physics, 69, 119, arXiv:astro-ph/0510487

Pepe, F. et al. 2004, A&A, 423, 385, arXiv:astro-ph/0405252

Pepliński, A., Artymowicz, P., & Mellema, G. 2008, MNRAS, 386, 179, arXiv:0709.3754

Pollack, J. B., Hubickyj, O., Bodenheimer, P., Lissauer, J. J., Podolak, M., & Greenzweig, Y. 1996, Icarus, 124, 62

Prilutskii, O. F., & Usov, V. V. 1976, Soviet Astronomy, 20, 2

Rasio, F. A., & Ford, E. B. 1996, Science, 274, 954

Rice, W. K. M., & Armitage, P. J. 2003, ApJ, 598, L55, arXiv:astro-ph/0310191

Safronov, V. S. 1969, Evoliutsiia doplanetnogo oblaka

Santos, N. C., Israelian, G., Mayor, M., Rebolo, R., & Udry, S. 2003, A&A, 398, 363, arXiv:astro-ph/0211211

Scharf, C. A. 2006, ApJ, 648, 1196, arXiv:astro-ph/0604413

Schulze-Makuch, D., & Irwin, L. N. 2002, Astrobiology, 2, 197

Seager, S., & Mallén-Ornelas, G. 2003, ApJ, 585, 1038, arXiv:astro-ph/0206228

Shakura, N. I., & Syunyaev, R. A. 1973, A&A, 24, 337

Shu, F. H., Adams, F. C., & Lizano, S. 1987, ARA&A, 25, 23

Sotnikova, N. Y., & Grinin, V. P. 2007, Astronomy Letters, 33, 594, 0809.4434

Spitzer, L. J. 1939, ApJ, 90, 675

Stempels, H. C., & Gahm, G. F. 2004, A&A, 421, 1159

Strand, K. A. 1943, PASP, 55, 29

Struve, O. 1952, The Observatory, 72, 199

Theuns, T., & David, M. 1992, ApJ, 384, 587

Trac, H., & Pen, U.-L. 2003, PASP, 115, 303, arXiv:astro-ph/0210611

van de Kamp, P. 1963, AJ, 68, 515

——. 1982, Vistas in Astronomy, 26, 141

van Zadelhoff, G.-J. et al. 2002, A&A, 395, 373, arXiv:astro-ph/0208503

Walder, R., & Folini, D. 2000, in Astronomical Society of the Pacific Conference Series, Vol. 204, Thermal and Ionization Aspects of Flows from Hot Stars, ed. H. Lamers & A. Sapar, 331–+

Ward, W. R. 1997, ApJ, 482, L211

Wolszczan, A. 1991, in Bulletin of the American Astronomical Society, Vol. 23, 1347

Wolszczan, A. 1994, Science, 264, 538

Wolszczan, A., & Frail, D. A. 1992, Nature, 355, 145

Woodward, P., & Colella, P. 1984, J. Comput. Phys., 54, 115